Quantifying the dominant sources of sediment in a drained lowland agricultural catchment: The application of a thorium-based particle size correction in sediment fingerprinting

Anthony Foucher, Patrick J. Laceby, Sébastien Salvador-Blanes, O. Evrard, Marion Le Gall, Irène Lefèvre, Olivier Cerdan, Vignesh Rajkumar, Marc Desmet

——Quantifying the dominant sources of sediment in a drained lowland agricultural catchment: the application of a thorium-based particle size correction in sediment fingerprinting

Anthony Foucher [a,*], J. Patrick Laceby [b], Sébastien Salvador-Blanes [a], Olivier Evrard [b], Marion Le Gall [b], Irène Lefèvre [b], Olivier Cerdan [c], Vignesh Rajkumar [a,d], Marc Desmet [a]

[a] E.A. 6293 GéHCO, GéoHydrosystèmes COntinentaux, Université F. Rabelais de Tours, Faculté des Sciences et Techniques, Parc de Grandmont, 37200 Tours, France

[b] Laboratoire des Sciences du Climat et de l'Environnement (LSCE/IPSL), UMR 8212 (CEA-CNRS-UVSQ), Avenue de la Terrasse, 91198 Gif-sur-Yvette Cedex, France

[c] Département Risques et Prévention, Bureau de Recherches Géologiques et Minières, 3 avenue Claude Guillemin, 45060 Orléans, France

[d] Centre for Water Resources, CEG, Anna University, Sardar Patel Rd, Chennai, Tamil Nadu 600025, India

*** Corresponding author:** Anthony.foucher@univ-tours.fr; Tel: (33) 247367090

Abstract

Soil erosion is one of the main factors influencing land degradation and water quality at the global scale. Identifying the main sediment sources is therefore essential for the implementation of appropriate soil erosion mitigation measures. Accordingly, caesium-137 (^{137}Cs) concentrations were used to determine the relative contribution of surface and subsurface erosion sources in a lowland drained catchment in France. As ^{137}Cs concentrations are often dependent on particle size, specific surface area (*SSA*) and novel Thorium (*Th*) based particle size corrections were applied. Surface and subsurface samples were collected to characterize the radionuclide properties of potential sources. Sediment samples were collected during one hydrological year and a sediment core was sampled to represent sediment accumulated over a longer temporal period. Additionally, sediment from tile drains was sampled to determine the radionuclide properties of sediment exported from the drainage network. A distribution modeling approach was used to quantify the relative sediment contributions from surface and subsurface sources. The results highlight a substantial enrichment in fine particles and associated ^{137}Cs concentrations between the sources and the sediment. The application of both correction factors reduced this difference, with the *Th* correction providing a more accurate comparison of source and sediment samples than the *SSA* correction. Modelling results clearly indicate the dominance of surface sources during the flood events and in the sediment core. Sediment exported from the drainage network was modelled to originate predominantly from surface sources. This study demonstrates the potential of *Th* to correct for ^{137}Cs particle size enrichment. More importantly, this research indicates that drainage networks may significantly increase the connectivity of surface sources to stream networks. Managing sediment transferred through drainage networks may reduce the deleterious effects of suspended sediment loads on riverine systems in similar lowland drained agricultural catchments.

Key Words*:* Sediment tracing, Agricultural lowland areas, Cesium-137, Particle size correction, Tile drainage networks

Highlights:

- Source and sediment caesium-137 activities were used to trace sediment sources
- Two particle size corrections were compared to address enrichment in fine particles
- A thorium-based correction out performed a specific surface area correction
- Sediment in this lowland agricultural catchment is supplied by surface sources
- Drainage networks may increase the connectivity of surface sources to rivers

1. Introduction

Soil erosion by water affects a significant proportion (16%) of agricultural land in Europe (Cerdan et al., 2010; Jones et al., 2012). Although natural, this degradation process is accelerated by land use change and anthropogenic pressures in agricultural landscapes (Bakker et al., 2008; Chartin et al., 2011; Sharma et al., 2011). Around the world, the negative effects of soil erosion are characterized by the decline of crop yields, the reduction of soil water storage capacity and decreases in soil organic matter (Berger et al., 2006; Boardman and Poesen, 2006). The main problems associated with accelerated soil erosion are often not only the actual soil loss itself, rather the adverse effects of elevated suspended sediment yields and adsorbed contaminants downstream (Walling et al., 2003).

The excess of fine sediment particles (e.g., <63 μm) associated with soil erosion are detrimental to water quality and stream environments (Kronvang et al., 2003; Owens et al., 2005; Horowitz, 2008). Elevated fine sediment loads can result in numerous problems such as elevated turbidity and reservoir siltation (Wood and Armitage, 1997; Nakamura et al., 2004). Importantly, fine sediments often transport contaminants such as heavy metals, Polychlorinated Biphenyls (PCB), phosphorus, pesticides, pathogens, and fallout radionuclides (Desmet et al., 2012; Ayrault et al., 2014; Evrard et al., 2014).

Currently, there is a limited understanding regarding the dominant sediment source in France in particular, and in drained lowland cultivated areas in general (Russell et al., 2001; Walling et al., 2002). The implementation of highly productive cropland agriculture practices in these regions has included the installation of drainage networks that induce a high level of connectivity between eroding soils and river systems. Although these land management changes were clearly associated with increased sediment yields (e.g Foster and Walling, 1994; Dearing and Jones, 2003; Ahn et al., 2008), the identification of the dominant sediment sources, their dynamics, and their pathways in drained landscapes with similar intensive agricultural practices remains poorly understood. Indeed, research has highlighted the limited information available regarding sediment exported through drainage networks in these environments (Kronvang et al., 1997; Walling and Collins, 2005; King et al., 2014).

To implement appropriate measures to reduce erosion and sediment production (Evrard et al., 2008), it is essential to identify the dominant sediment sources and understand their dynamics. Sediment fingerprinting techniques provide a direct method to identify and quantify sediment contributions from different sources (Collins and Walling, 2002). The technique is based on the direct comparison of sediment and source properties (Walling et al., 1993; Collins et al., 2010). A variety of parameters have been used in sediment fingerprinting studies to discriminate between potential sources, including geochemical composition, sediment color, plant pollen, and fallout radionuclides (Brown, 1985; Walling et al., 2002; Martinez-Carreras et al., 2010). In particular, caesium-137 (^{137}Cs)

discriminates between surface and subsurface soils, regardless of other soil properties including catchment geology (Wallbrink et al., 1996; Walling, 2005; Caitcheon et al., 2012).

^{137}Cs ($t_{1/2}$ = 30 years) is an artificial radionuclide originating from two main sources in Western Europe: thermonuclear weapons testing (1950–1970s) and the Chernobyl accident. Fallout from the Fukushima accident in 2011 was shown to be negligible in this region (Evrard et al., 2012). ^{137}Cs is quickly and predominantly fixed to fine particles (He and Walling, 1996; Wallbrink and Murray, 1996; Motha et al., 2002). In undisturbed soils, ^{137}Cs is concentrated near the soil surface (i.e. within the top 10 cm), with concentrations decreasing exponentially with depth (Matisoff et al., 2002). In cultivated soils, ^{137}Cs concentrations are homogenized by tillage (He and Walling, 1997; Matisoff et al., 2002; Chartin et al., 2011). Accordingly, sediment generated from subsoil erosion processes, such as channel bank erosion, will have low ^{137}Cs concentrations, whereas sediment generated from surface soils will have elevated ^{137}Cs concentrations (e.g Caitcheon et al., 2012; Olley et al., 2013). Through comparing sediment and source ^{137}Cs concentrations, it is possible to determine whether sediment is derived from surface or subsurface sources.

Soil erosion processes result in the preferential mobilization and transfer of fine sediment particles (He and Walling, 1996). To reduce the impacts of grain size selectivity, many fingerprinting studies isolate either the <10 µm (Olley and Caitcheon, 2000; Wallbrink, 2004) or the <63 µm fraction (Navratil et al., 2012; Pulley et al., 2015) to mitigate differences in the particle size distributions of source soil and sediment. To further reduce the grain size effect when tracing sediment, a correcting factor has been applied (Collins et al., 1996). This correction is based on the specific surface area (*SSA*) of sediment and source soils, and it relies on the assumption of positive linearity between *SSA* and tracer property concentrations. Linear particle size correction factors may be useful when there is a narrow range of particle size differences between source soils and sediment (Koiter et al., 2013). This particle size correction has been applied to various tracers, such as radionuclides (He and Owens, 1995; He and Walling, 1996), phosphorus (Owens and Walling, 2002) and extractable metals (Horowitz and Elrick, 1987).

Although this particle size correction has been widely applied (Collins et al., 2001; Carter et al., 2003), there are acknowledged limitations (Koiter et al., 2013). For example, Smith and Blake (2014) demonstrated that the most critical assumption, which could have large effects on source apportionments, is the hypothesis of positive linearity between particle size and tracer concentration. Contrary to previous studies, Smith and Blake (2014) demonstrated that this relationship does not apply to all tracer properties and that the assumption of linearity must be routinely tested. Russell et al. (2001) also demonstrated that the linear particle size correction relationship was inappropriate when there were large *SSA* differences between sources.

Given the potential uncertainty associated with the *SSA* correction, some authors, such as Martinez-Carreras et al. (2010), do not apply it. As an alternative to the *SSA*-derived correction, Sakaguchi et al. (2006) demonstrated the potential of a Thorium (*Th*) normalization to correct for the

144 grain size effect in lake sediment cores. Owing to its measurement in gamma spectrometry along with
145 ^{137}Cs, there is a novel utility in the potential for *Th* to correct for grain size differences that could
146 remove the need for simultaneous *SSA* measurements in sediment fingerprinting studies using fallout
147 radionuclides for source discrimination.
148 The objective of this research is to identify the dominant sediment sources and their temporal
149 variation in the Louroux catchment, France; a small agricultural catchment, representative of the
150 lowland drained landscapes of Western Europe. To determine the main source of sediment in the
151 Louroux catchment, first we examine particle size effects and compare the impacts of *Th* and *SSA*
152 corrections on ^{137}Cs soil and channel bank concentrations. Second, we characterize the ^{137}Cs
153 concentrations of surface and subsurface sources. Third, we model the relative contribution of these
154 sources to sediment sampled throughout a year, a sediment core collected in a pond at the outlet of the
155 catchment, and sediment sampled within the tile drainage network.
156

157 # 2. Materials and methods

158

159 ## *2.1. Study area*

160

161 The Louroux pond catchment (24 km²) is a headwater agricultural basin located in the central
162 part of the Loire River basin, France (Fig. 1). The catchment is characterized by a flat topography
163 (average slope 0.44%; altitude ranging from 94 to 129 m). The catchment surface is primarily
164 occupied by arable land (78%), followed by pasture (18%) and forest (4%) (European Environment
165 Agency, 2002). The climate is temperate oceanic with a mean annual rainfall of 684 mm (between
166 1971–2000). The bedrock consists of carbonates, detrital and loess deposits (Rasplus et al., 1982).
167 Soils are classified as Epistagnic Luvic Cambisols, which are predominantly hydromorphic and prone
168 to surface crusting (Froger et al., 1994).
169 This basin, like the majority of the great western agricultural plain in Europe, has undergone a
170 global modernization of agricultural practices and land use changes. Two land consolidation schemes
171 were implemented in the catchment in 1954 and 1992. Stream networks were created or redesigned,
172 and tile drainage networks were installed to drain the hydromorphic soils.
173 The Louroux pond, located at the catchment outlet (52 ha; Fig. 1), was created during the
174 Middle-Ages (1000 AD). Recent research indicated that a significant increase in soil erosion in the
175 catchment during the last 70 years resulted in the accelerated sedimentation and eutrophication of the
176 pond (Foucher et al., 2015). Over the last decade, the Louroux pond has received an annual average
177 input of 2500 tons of terrigenous material (Foucher et al., 2015).
178

179 ## *2.2 Sampling*

180

181 *2.2.1. Soil and stream bank sampling*

182 Soil samples from ground surfaces and subsurface material exposed on actively eroding river
183 banks were collected from January 2013 to February 2014. Sampling was restricted to cropland areas,
184 as soil erosion was shown to be negligible under grassland in similar environments of Northwestern
185 Europe (Cerdan et al., 2002; Evrard et al., 2010). In addition, grassland areas in this catchment are
186 ploughed approximately every 10 years, mixing ^{137}Cs in the soil profile similarly to croplands.

187 Surface sources (n = 34) were sampled by scraping the top 2–3 cm layer of soil with a plastic
188 spatula in potentially eroding areas directly connected to the stream network. Each of these surface
189 source composite samples was comprised of five sub-samples collected within an area of 5 m².
190 Subsurface sources (n = 15) were sampled by scraping a 2–3 cm layer of the actively eroding bank
191 face. In addition, sediment was collected in hillslopes during the rain by placing plastic bottles on the
192 hillslope surface to sample sediment during runoff events (n = 3). These plastic bottles were collected
193 after events along with the deposited sediment.

194

195 *2.2.2. Suspended sediment sampling*

196 Hydro-sedimentary parameters were continuously recorded at five automated monitoring sites
197 (S1–S5, Fig. 1). Water discharge was measured using a v-notch weir. Suspended sediment was
198 continuously measured using a Ponsel® calibrated turbidity sensor. Twenty-four liters of river water
199 were automatically collected according to the water level at each station during five flood events (n =
200 21) and once during the low-water period (n = 4) to examine variability throughout the hydrological
201 year in 2013–2014. All individual samples for each station and for each flood were mixed to prepare
202 composite samples. In addition to the river monitoring sites, three stations were installed at tile drain
203 outlets to characterize the properties of the material transiting through the drainage networks and to
204 determine if sediment exported from this network had ^{137}Cs concentrations similar to surface or
205 subsurface sources (Fig. 1). To characterize the origin of sediment accumulated over a longer temporal
206 period (2003–2013) at the catchment outlet (Fig. 1), the top 10 cm of a 110 cm long core collected in
207 March 2013 was subsampled in 3 cm increments. This sediment core was sampled in the central pond
208 depression, an area that is representative of sediment deposition in the Louroux Pond. More details on
209 the core sampling and fallout radionuclide dating are provided in Foucher et al. (2015).

210

211 *2.3. Sample treatment and analysis*

212

213 Suspended sediment concentrations for the composite samples were determined by weighing
214 after filtration (40 microns acetate filters). Particle size analyses were performed on all suspended
215 sediment samples as well as on randomly selected source samples (n = 18) after removing carbonates

and organic material with hydrogen peroxide. Particle size was analysed with laser granulometry (Malvern Mastersizer®) characterizing the textural parameters ranging between 0.01 and 3500 µm.

Randomly selected subsamples of subsurface (n = 5) and surface sources (n = 5) were sieved to determine radionuclide activities in different particle size fractions. Samples were mechanically sieved to 63 and 50 µm. The <20 µm fraction was then isolated by using the settling velocity relationship predicted by Stokes′ Law. These analyses were used to calculate the difference between the bulk samples and the sieved samples, and to examine the utility of the two different corrections.

Suspended sediments collected during the flood events were flocculated using calcium hydroxide ($CaOH_2$), to recover and concentrate radionuclides. For the measurement of radionuclides, ~80 g of material was analysed for source samples and ~10 g for sediment samples. Activities were determined by gamma spectrometry using low background coaxial N and P type GeHP detectors (Canberra/Ortec) at the Laboratoire des Sciences du Climat et de l'Environnement (France) (Evrard et al., 2011). Radionuclides activities were decay-corrected to the sampling date. In addition to the radionuclide measurement, *Th* concentrations expressed in ppm were calculated from ^{228}Th activity concentrations. Only ^{137}Cs is modelled in this study as only one tracer is required to discriminate between two sources.

2.4. Particle size corrections

To limit the bias potentially introduced by particle size difference between sources and sediment, a correcting factor used by Collins et al. (1996) was applied to radionuclide activities. This approach is based on the ratio of *SSA* of each individual sediment sample to the mean *SSA* of each source type, multiplied by the mean activity for each source:

$$SSA\ correcting\ factor_i = \frac{(SSA_i)}{(SSA_y)} \times T_y \quad (1)$$

where SSA_i = specific surface area for each individual sample (i), SSA_y = specific surface area for each source type (y), and T_y = mean tracer concentration for each source type (y).

The *Th* content correction was calculated based on the ratio of the radionuclide concentration normalized with ln(*Th*) of each individual sample, to the mean radionuclide concentration normalized with ln(*Th*) of each source type, multiplied by the mean radionuclide concentration of each source:

$$\ln(Th)\,correcting\ factor_i = \frac{T_i / \ln(Th)_i}{T_y / \ln(Th)_y} \times T_y \quad (2)$$

where T_i = the tracer concentration for each individual sample (i), $\ln(Th)_i$ = the logarithm of the *Th* concentration (in ppm) for each individual sample (i), and $\ln(Th)_y$ = the logarithm of the *Th* concentration (in ppm) for each source type (y).

The *SSA* and *Th* corrections were applied for randomly selected soil (n = 10) and channel bank samples (n = 7) to test the relationship between the corrected and measured ^{137}Cs values. These results were then used to calculate the corrected values of ^{137}Cs with the *SSA* and *Th* correction factors of Eqs. (1) and (2). These corrected and measured values are first plotted to deduce equations from these relationships. These relations are then used to correct the entire dataset for each source type and for both correction techniques. To check the applicability of these corrections, sediment samples were collected on hillslopes during different hydrological periods and the ^{137}Cs activities measured for these samples were compared to these corrected values.

2.5. Distribution modelling

Distribution modelling approaches have been recently applied to sediment tracing research analyzing fallout radionuclides and elemental geochemistry (Caitcheon et al., 2012; Olley et al., 2013; Laceby and Olley, 2015). This modelling approach incorporates distributions throughout the entire modelling framework, including the relative contribution terms (i.e. not only source and in-stream components).

To determine the relative source contribution to in-stream sediment, it is assumed that the sediment samples are derived from a discrete mixture of sources with surface sources contributing x and subsurface sources contributing $1 - x$. With the distribution modelling approach, x is modelled as a truncated normal distribution ($0 \leq x \leq 1$), with a mixture mean (μ_m) and standard deviation (σ_m). Distributions of ^{137}Cs activities in surface (A) and subsurface (B) sources are then modelled when determining the relative source contributions (x) to in-stream sediment based on the following equation:

$$Ax + B\,(1-x) = C \quad (3)$$

where C is the in-stream sediment distribution. Normal distributions were modelled for source and sediment distributions as Laceby and Olley (2015) demonstrated that they resulted in more accurate modelling results compared to Student's t distributions. Sediment collected from the core sample from the Louroux Pond and sediment obtained from the tile drainage network were first individually

285 modelled. Second, distributions were modelled for sediment sample groups for different flood events
286 and also the different monitoring stations.
287 The model was optimized with the Optquest algorithm in Oracle's Crystal Ball software. For
288 more details on the modelling approach, see Laceby and Olley (2015). In general, the optimal value of
289 x was determined by simultaneously solving Eq. (3) 2500 times with the Optquest algorithm. During
290 this simulation, 2500 Latin hypercube samples were drawn from the source (A and B) and in-stream
291 sediment (C) distributions while solving Eq. (3) by varying x, μ_m and σ_m. This simulation was then
292 repeated an additional 2500 times with the median of x for these additional simulations being reported
293 as the surface source proportional contribution to sampled sediment.
294 The model uncertainty for each sources' proportional contribution is calculated by summing
295 the modelled $\sigma_{m,}$ with the median absolute deviation (MAD) of $\sigma_{m,}$, and also the MAD of the modelled
296 source proportional contributions. The latter two components of model error are calculated from the
297 additional 2500 simulations. This model uncertainty combines actual σ_m for each source contribution
298 with the MAD of this standard deviation and the MAD of the actual source contribution (x) for the
299 additional 2500 simulations.
300
301
302 # 3. Results
303
304 ## *3.1. Correction of grain size effects*
305
306 Particle size analyses highlight differences between the D_{50} (median particle size) of the
307 surface (32.2 ± 7 µm) and subsurface sources (38.5 ± 8 µm) in comparison to the in-stream sediment
308 (6.2 ± 2 µm). A t-test between the two sources did not show a significant difference between their D_{50}
309 (p-value = 0.14). Significant differences were found between D_{50} of surface sources and in-stream
310 sediment (p = 0.00) and also between subsurface sources and in-stream sediment samples (p = 0.00).
311 In addition, soil samples collected before and during runoff events clearly highlight the particle size
312 enrichment during sediment generation processes, with an average activity measured before the runoff
313 of 3.7 ± 3 Bq kg^{-1} compared to 17 ± 3 Bq kg^{-1} during runoff. These samples demonstrate a difference
314 of 78% between surface sources and generated sediment, with an enrichment factor of 4.6.
315 The significant particle size effect noted above may prevent the direct comparison between
316 bulk sources and sediment samples. To test the impact of this effect on radionuclide activities, several
317 source samples were fractionated. The results from five soil samples highlight an enrichment factor of
318 2 between the bulk and the <20 µm particle size fraction for the soil samples and the absence of
319 detectable ^{137}Cs in the 20-50 µm fraction for these samples (Fig. 2). There is an 80% difference
320 between the bulk and sediment particle size which can impact modelling results. For the 63 µm

fraction, this difference is reduced to 77% compared to 64% for the 20 µm fraction. Isolating the <20 µm fraction does not allow for a direct comparison between the sources and the suspended sediment. The particle size enrichment of ^{137}Cs concentrations is plotted in Fig. 3 demonstrating clearly that sediment samples collected during the flood events are distinct from the source soils. To address this particle size effect and allow for comparison between sources and sediment samples, source activities were corrected with two distinct particle size proxies.

SSA, *Th* and ^{137}Cs activities measured for soil (n = 10) and channel bank samples (n = 7) were plotted to deduce the relationships between the corrected and measured values (Fig. 4). These plots demonstrate that for the *SSA* correction a strong linear relationship exists between the corrected values and measured ^{137}Cs activities in the soil (r^2 = 0.89) and channel bank samples (r^2 = 0.94) (Fig. 4). The *Th* particle size correction, based on ln(*Th*) normalization, also had a strong exponential relationship for the channel bank samples (r^2 = 0.98) and surface soil samples (r^2 = 0.96). Both corrections have a similar relationship for the subsurface samples. In contrast, the relationship obtained for the surface samples was different. The ^{137}Cs activities after the *SSA* correction ranged between 3.2 and 20 Bq kg^{-1} whereas the ^{137}Cs activities after the *Th* normalization ranged between 1 and 30 Bq kg^{-1}. For both approaches, the mean values are comparable, 9.3 and 10.2 Bq kg^{-1} for the *SSA* and *Th* corrections respectively. The difference was the wider range with the *Th* correction.

As particle size data were available for only part of the dataset, both correcting factors were applied to the whole data set (subsurface sources n = 15 and surface sources n = 34) by using the equations for the surface and subsurface samples shown in Fig. 4. The corrected data are plotted with ^{210}Pb$_{ex}$ in Fig. 5. After the application of both corrections, sediment ^{137}Cs activities generally plotted within the ^{137}Cs activity range of the potential sources. With the *SSA* correction, five sediment samples remain outside the source range (black squares in Fig. 5), whereas with the *Th* correction only one sample plots outside the source range. Therefore, the *Th* correction likely provides a more direct comparison with the sediment samples than the *SSA* correction.

3.2. ^{137}Cs concentration in source samples

Activities in the samples collected from stream banks range between 0 ± 0.3 and 3.1 ± 0.2 Bq kg^{-1} with an average of 1.2 ± 0.2 Bq kg^{-1}. Soil surface activities range between 1 ± 0.1 and 7.9 ± 0.2 Bq kg^{-1} with an average of 3.2 ± 0.2 Bq kg^{-1}. These potential sources are statistically different (p = 0.00).

After the application of the *SSA* correction, the subsurface sample activities range between 0.7 and 5.1 Bq kg^{-1} (mean: 1.7 Bq kg^{-1}). These sample activities, after the *Th* correction, range between 0 and 6.5 Bq kg^{-1} (mean: 1.8 Bq kg^{-1}). The surface sample concentrations are more variable, ranging between 3.7 and 23.8 Bq kg^{-1} (mean: 10 Bq kg^{-1}) after the *SSA* correction and between 0.8 and 35.5 Bq

357 kg^{-1} (mean: 11.2 Bq kg^{-1}) after the *Th* correction. Summary statistics of ^{137}Cs concentrations are
358 provided in Table 1.
359 The fitted normal distributions for surface and subsurface sources with both particle size
360 corrections are plotted in Fig. 6. The source samples are plotted in rank order. The source distribution
361 areas overlap only by 25% with the *SSA* correction compared to 62% with the *Th* correction. These
362 distributions are used to model the proportional contribution of the potential sources to suspended
363 sediment, the core samples, and the drainage network samples.
364
365 *3.3. ^{137}Cs concentration in sediments samples*
366
367 Activities of ^{137}Cs for the 23 sediment samples collected over the hydrological year range
368 between 6.1 ±1 and 36.7 ± 4.7 Bq kg^{-1} with an average of 18.4 ± 3.4 Bq kg^{-1}. The highest ^{137}Cs
369 activities have been recorded at the Masnier (station 3) and Grand Bray rivers (station 2) with average
370 ^{137}Cs activities of 19 ± 4.9 and 22.4 ± 4.3 Bq kg^{-1}, respectively. For the other stations, ^{137}Cs activities
371 were similar (17.7 ± 3.6, 16.7 ± 2 and 15.5 ± 2.1 Bq kg^{-1} for stations 1, 4 and 5). The flood event on
372 January 29, 2014 had the highest activity of all floods, with an average activity of 24.7 ± 2.8 Bq kg^{-1}
373 followed by the flood of April 4, 2014 (19.8 ± 7.3 Bq kg^{-1}). The two floods sampled on December 29,
374 2013 and February 13, 2014 were similar, with ^{137}Cs concentrations ranging between 17.1 ± 1.1 and
375 17 ± 4.3 Bq kg^{-1} respectively. Samples collected during the low-flow periods are characterized by low
376 ^{137}Cs activities (6.9 ± 0.8 Bq kg^{-1} on September 10, 2013 and 13.9 ± 12.3 Bq kg^{-1} on April 30, 2014).
377 The sediment collected at the tile drain outlets (n = 5) were characterized by the presence of high ^{137}Cs
378 activities with an average of 23.4 ± 4 Bq kg^{-1} (ranging between 8.6 ± 0.3 and 30.6 ± 0.5 Bq kg^{-1})
379 indicative of elevated surface source contributions. As shown in Fig. 5, these high concentrations of
380 ^{137}Cs in the sediment samples mainly plot within the concentration range of surface sources. Over a
381 10-year period (2003–2013) the ^{137}Cs activity of material accumulated in the pond ranged between
382 10.9 ± 0.7 and 11.9 ± 0.7 Bq kg^{-1} with an average activity at the upper 10 cm of the core being 11.4 ±
383 0.5 Bq kg^{-1}. These values also plot clearly within the surface source range. Summary statistics of ^{137}Cs
384 concentrations are provided in Table 2 for all sediment samples.
385
386 *3.4. Modelling results – source identification*
387
388 When all sediment samples from the monitoring stations are grouped together (*C* in Eq. (3)),
389 the modelling results for both corrections indicate that sediment transported in the Louroux catchment
390 are almost entirely originated from surface sources (99 ± 1.2% with the *SSA* correction and 94 ± 1.5%
391 with the *Th* correction). Corrected ^{137}Cs activities in sediment collected at the different monitoring
392 stations clearly plots within the distribution of surface source ^{137}Cs activities (Fig. 7). The modelling
393 results averaged for the 5 monitoring stations indicate a surface contribution of 99% (± 0.5%) with the

394 *SSA* correction. The results with the *Th* correction are comparable with a mean modelled surface
395 contribution of 98% (± 1.9%). The mean difference between surface source contributions with the *SSA*
396 and *Th* corrections modelled for all monitoring stations was 1.2% (± 1.6%). Table 3 lists all modelling
397 results.

398 To further examine sediment sources in this catchment, the different events sampled were
399 modelled separately. Sediment samples collected during flood events have elevated ^{137}Cs
400 concentrations (suspended sediment samples SSE2–6 in Fig. 8). These high activities indicate a major
401 contribution of surface material during the flood events. The modelled results indicate a surface source
402 contribution of 99% (± 0.4%) with the *SSA* correction and 99% (± 0.5%) with the *Th* correction.
403 Samples collected during a low flow event had a ^{137}Cs signature clearly lower than during the flood
404 conditions representative of a more homogeneous mixture of surface and subsurface sources (SSE1 in
405 Fig. 8). During the low flow period, the sediment distribution plotted closer to the subsurface source
406 distribution (Fig. 8). Surface sources were modelled to contribute 49% (± 3.5%) with the *SSA*
407 correction compared to 40% (± 2.1%) with the *Th* correction. Although there was a 9% difference
408 between the modelled results with the *SSA* and *Th* corrections for the low flow event, the mean
409 difference between the modelled surface source contributions for all events was only 2% (± 3%).

410 The mean ^{137}Cs value of sediment at the tile drainage network outlet (23.4 ± 4 Bq kg^{-1}) was
411 higher than during the floods (18.4 ± 3.4 Bq kg^{-1}), (Figs. 6 and 7). Sediment exported from the
412 drainage network was modelled to originate predominantly from surface sources (99 ± 2.5%) with
413 both corrections (Fig. 9). This indicates that these drainage networks potentially facilitate the transfer
414 of surface soils and should be treated as a surface source in this catchment. For the sediment core,
415 results indicate that sediment is mainly derived from surface sources with a modelled contribution of
416 99% (± 1.5%) with the *SSA* correction compared to 97% (± 6.7%) with the *Th* correction.

417

418 # 4. Discussion

419

420 In this study the *SSA* and *Th* corrections reduced particle size enrichment impacts on ^{137}Cs
421 concentrations. The *SSA* measured for both sources were similar (subsurface mean: 340 m² kg^{-1},
422 surface mean: 390 m² kg^{-1}). The significant difference between sediments and source *SSA* is
423 potentially indicative of particle size enrichment during sediment mobilization and transport processes.
424 This enrichment is highlighted by the large observed particle size difference between sources and
425 sediment. The application of both particle size corrections clearly improved the relationship between
426 sediment and their sources. When examining all modelling results, there was only a mean difference of
427 2% (± 3%) between both corrective approaches. There was only one exception, the low flow sediment
428 sample (SSE1) where modelling approaches differed by 9%.

The main observed difference between the *Th* and *SSA* corrections could be because the application of the *Th* correction allows a broader range of values than the *SSA* approach. Nevertheless, the high values for the surface sources obtained with the *Th* correction do not seem to be outliers as the drain samples have higher ^{137}Cs activities. By comparison at the sample scale, the *Th* correction is more applicable than the *SSA* correction. The application of the *Th* correction to the surface source samples (measured ^{137}Cs activity: 3.7 ± 3 Bq kg^{-1}) changed the surface source ^{137}Cs activity to 14.3 Bq kg^{-1} compared to 11.4 Bq kg^{-1} with the *SSA* correction. The average ^{137}Cs activities during runoff was 17 ± 3 Bq kg^{-1}. The application of both corrections could be improved by collecting additional sediment and source samples covering a wider range of ^{137}Cs activities.

The modelling results for sediment samples taken over the entire hydrological year (2013/2014) and for the sediment core clearly illustrate that surface sources dominate the supply of sediment in this catchment (μ = 97% ± 6.7% for the sediments and 99 ± 1.5% for the sediment core). These results are in agreement with the review on sediment sources in British rivers that indicated surface sources dominate the supply of sediment, accounting for between 60% and 96% of the sediment yields, with 85–95% being typical (Walling, 2005).

The sediment exported by the drainage network is characterized by higher ^{137}Cs activities than the soil samples (3.2 ± 0.2 Bq kg^{-1} for average soil samples and 23.4 ± 4 Bq kg^{-1} for drainage network sediment). These high values are worthy of attention because ^{137}Cs activity concentrations are expected to decrease below the plough depth in cultivated soil (He and Walling, 1997) and are nearly undetectable in subsurface soil (Matisoff et al., 2002). One possibility could be that there has been ^{137}Cs migration down in the soil profile in our catchment. According to previous studies (Sogon et al., 1999; Walling et al., 2002; Chapman et al., 2005), macropores are a potential link between the topsoil with high ^{137}Cs activities and the drainage networks. These macropores can be induced by the soil properties, agricultural soil works, and vegetal activities (Oygarden et al., 1997), and they can be a preferential pathway of sediment originating from the topsoil and labelled with ^{137}Cs (Jagercikova et al., 2014). This direct pathway offers the best explanation for the rapid sediment transport observed by Chapman et al. (2005) and potentially the high ^{137}Cs activities observed in sediment sampled in our studied drainage network.

Another explanation is that eroded surface material is being exported through the drainage network. Similarly to Walling et al. (2002), sediment samples from the studied field drains have higher ^{137}Cs activities than the soil samples. This radionuclide enrichment at the drainage network outlet has also been described by Sogon (1999) who demonstrated the occurrence of preferential particle size selection in the upper soil and the migration of the finest particles through the tile drainage network during runoff events. A combination of these factors likely explains this particle selectivity between soil and drain material and additional research is required to determine the dominant transfer mechanisms.

There are limited analyses of sediment contributions from drainage networks available in France (Penven and Muxart, 1995; Sogon et al., 1999; Penven et al., 2001). Research from other countries demonstrated that drainage networks provide a significant contribution to sediment export. In the UK, drainage networks were clearly an important source to sediment yields accounting for between 27% and 55% of sediment exported (Russell et al., 2001; Walling et al., 2002). Furthermore, Foster et al. (2003) reported that drainage networks contributed more than 50% of sediment. At the global scale, drainage network contributions may be significant. For instance, Macrae et al. (2007) estimated >42% of annual hydrological discharge is originated from the drainage network in a Canadian agricultural catchment. According to King et al. (2014), this hydrological pathway is under-studied in agricultural basins. More research is required in the study area to determine whether ^{137}Cs has migrated down through the soil profile or whether these drainage networks simply act as conduit for quick transportation of surface soils to the stream network during runoff events.

At the global scale, previous sediment fingerprinting studies demonstrated that subsurface contribution to sediment yields varied among catchments depending on several parameters such as morphology and land use. Data compiled by Walling and Collins (2005) indicate that generally bank erosion can contribute between 5% and 15% of sediment exported in British rivers but in some cases it can exceed 40%. In the review of Haddadchi et al. (2013), subsurface erosion from channel bank sources was reported to contribute typically between 15% to 30% of suspended sediment load. In Australian catchments, it is not uncommon for subsurface sources to contribute more than 90% of sediment load (Caitcheon et al., 2012; Olley et al., 2013; Laceby et al., 2015). Our results remain in agreement with European studies, with an average riverbank contribution ranging between 11% to 32% for the last decade.

In the Louroux catchment, the majority of the sediments are exported during the flood events. Modelling results indicate the dominance of the surface sources during these events whereas samples collected during the lower flow periods have an increased proportion of sediments derived from subsurface sources. The volume of water and sediment exported during the low flow events is often insignificant compared to the volume of sediment exported during flood events, though more research is required to define the relative proportion of both sources during the entire hydrological year.

5. Conclusions

This study highlights the potential of *Th* based particle size corrections. The application of this correcting factor produced globally better results that the *SSA* correction. There remains, however, more experimentation required to test the validity of this approach to particle size correction in various environments, particularly catchments with heterogeneous geologies where *Th* may be a significant discriminator between different spatial sediment sources.

Modelling results indicate that sediment transported during the flood events in the Louroux catchment are almost entirely originated from surface sources, regardless of the correcting factor employed (~ 99%). During these events, two pathways can mobilize this surface source: sheet and rill erosion associated with the runoff events and the sediment exported from the drainage network which was modelled to originate predominantly from surface sources (99% ± 2.5%). During the low flow period, modelling results correspond to a more homogenous mixture between surface and subsurface sources with contributions of subsurface source ranging between 51% and 60%.

Over the last 10 years, surface sources dominated the supply of sediment with both corrections in the pond (99% ± 1.5% to 97% ± 1.5%). Accordingly, management of deleterious sediments with contaminants accumulated within the Louroux pond should focus on reducing the supply of sediment from surface sources. Future research should examine the efficacy of drainage networks for connecting sediments from surface sources to the stream network in more detail. Managing sediment transferred through drainage networks may reduce suspended sediment loads in similar lowland agricultural catchments.

Acknowledgements

The authors thank Xavier Bourrain and Jean-Noël Gautier for their advice and technical support. Support from Aurelia Mathieu, Jean-Paul Bakyono and Rosalie Vandromme with soil and sediment sampling is gratefully acknowledged. This work was supported by grants from the Loire-Brittany Water Agency (TrackSed and Drastic projects). The authors would also like to thank the anonymous reviewers for their constructive comments.

References

Ahn, Y., Nakamura, F., Mizugaki, S., 2008. Hydrology, suspended sediment dynamics and nutrient loading in Lake Takkobu, a degrading lake ecosystem in Kushiro Mire, northern Japan. Environmental Monitoring and Assessment, 145, pp. 267-281.

Ayrault, S., Le Pape, P., Evrard, O., Priadi, C.R., Quantin, C., Bonté, P., Roy-Barman, M., 2014. Remanence of lead pollution in an urban river system: a multi-scale temporal and spatial study in the Seine River basin, France. Environmental Science and Pollution Research, 21(6), 4134-4148.

Bakker, M.M., Govers, G., van Doorn, A., Quetier, F., Chouvardas, D., Rounsevell, M., 2008. The response of soil erosion and sediment export to land-use change in four areas of Europe: The importance of landscape pattern. Geomorphology, 98(3-4), pp 213–226.

Berger, G., Kaechele, H., Pfeffer, H., 2006. The greening of the European common agricultural policy by linking the European-wide obligation of set-aside with voluntary agri-environmental measures on a regional scale. Environmental Science & Policy 9(6), pp 509-524.

Boardman, J., Poesen, J., 2006. Soil erosion in Europe: major processes, causes and consequences. In: J.Boardman and J. Poesen (Editors), Soil erosion in Europe. Wiley, Chicester. pp. 479-489.

Brown, A., 1985. The potential use of pollen in the identification of suspended sediment sources. Earth Surface Processes and Landforms, 10, 27 - 32.

Caitcheon, G.G., Olley, J.M., Pantus, F., Hancock, G., Leslie, C., 2012. The dominant erosion processes supplying fine sediment to three major rivers in tropical Australia, the Daly (NT), Mitchell (Qld) and Flinders (Qld) Rivers. Geomorphology, 151-152(No), pp 188-195.

Carter, J., Owens, P.N., Walling, D.E., Leeks, G.J.L., 2003. Fingerprinting suspended sediment sources in a large urban river system. Science of The Total Environment, 314-316(0), pp. 513-534.

Cerdan, O., Bissonnais, Y.L., Souchère, V., Martin, P., Lecomte, V., 2002. Sediment concentration in interrill flow: interactions between soil surface conditions, vegetation and rainfall. Earth Surface Processes and Landforms, 27(2), pp. 193-205.

Cerdan, O., Govers, G., Le Bissonnais, Y., Van Oost, K., Poesen, J., Saby, N., Gobin, A., Vacca, A., Quinton, J., Auerswald, K., Klik, A., Kwaad, F.J.P.M., Raclot, D., Ionita, I., Rejman, J., Rousseva, S., Muxart, T., Roxo, M.J., Dostal, T., 2010. Rates and spatial variations of soil erosion in Europe: A study based on erosion plot data. Geomorphology, 122(1-2), 167-177.

Chapman, A.S., Foster, I.D.L., Lees, J.A., Hodgkinson, R.A., 2005. Sediment delivery from agricultural land to rivers via subsurface drainage. Hydrological Processes, 19(15), pp 2875-2897.

Chartin, C., Evrard, O., Salvador-Blanes, S., Hinschberger, F., Van Oost, K., Lefèvre, I., Daroussin, J., Macaire, J.-J., 2011. Quantifying and modelling the impact of land consolidation and field borders on soil redistribution in agricultural landscapes (1954-2009). CATENA, 110(0), 184-195.

Collins, A.L, Walling, D.E., Leeks, G.J.L., 1996. Composite fingerprinting of the spatial source of fluvial suspended sediment : a case study of the Exe and Severn river basins, United Kingdom. . Géomorphologie : relief, processus, environnement, 2(2), pp. 41-53.

576 Collins, A.L., Walling, D.E., Sichingabula, H.M., Leeks, G.J.L., 2001. Suspended sediment
577 source fingerprinting in a small tropical catchment and some management
578 implications. Applied Geography, 21(4), pp. 387-412.
579 Collins, A.L., Walling, D.E., 2002. Selecting fingerprint properties for discriminating
580 potential suspended sediment sources in river basins. Journal of Hydrology, 261, 218 -
581 244.
582 Collins, A.L., Zhang, Y., Walling, D.E., Grenfell, S.E., Smith, P., 2010. Tracing sediment loss
583 from eroding farm tracks using a geochemical fingerprinting procedure combining
584 local and genetic algorithm optimisation. Science of The Total Environment, 408(22),
585 pp 5461–5471.
586 Dearing, J.A., Jones, R.T., 2003. Coupling temporal and spatial dimensions of global
587 sediment flux through lake and marine sediment records. Global and Planetary
588 Change, 39(1-2), pp. 147-168.
589 Desmet, M., Mourier, B., Mahler, B.J., Van Metre, P.C., Roux, G., Persat, H., Lefèvre, I.,
590 Peretti, A., Chapron, E., Simonneau, A., Miège, C., Babut, M., 2012. Spatial and
591 temporal trends in PCBs in sediment along the lower Rhône River, France. Science of
592 The Total Environment, 433(0), 189-197.
593 European Environment Agency, 2002. EEA-ETC/TE. 2002. CORINE land cover update.
594 I&CLC2000 project. Technical guidelines, http://terrestrial.eionet.eu.int.
595 Evrard, O., Vandaele, K., van Wesemael, B., Bielders, C.L., 2008. A grassed waterway and
596 earthen dams to control muddy floods from a cultivated catchment of the Belgian loess
597 belt. Geomorphology, 100(34), 419-428.
598 Evrard, O., Nord, G., Cerdan, O., Souchère, V., Le Bissonnais, Y., Bonté, P., 2010. Modelling
599 the impact of land use change and rainfall seasonality on sediment export from an
600 agricultural catchment of the northwestern European loess belt. Agriculture,
601 Ecosystems & Environment, 138(1-2), pp. 83-94.
602 Evrard, O., Navratil, O., Ayrault, S., Ahmadi, M., Némery, J., Legout, C., Lefèvre, I., Poirel,
603 A., Bonté, P., Esteves, M., 2011. Combining suspended sediment monitoring and
604 fingerprinting to determine the spatial origin of fine sediment in a mountainous river
605 catchment. Earth Surface Processes and Landforms, 36, 1072-1089.
606 Evrard, O., Van Beek, P., Gateuille, D., Pont, V., Lefèvre, I., Lansard, B., Bonté, P., 2012.
607 Evidence of the radioactive fallout in France due to the Fukushima nuclear accident.
608 Journal of environmental radioactivity, 114, 54-60.
609 Evrard, O., Chartin, C., Onda, Y., Lepage, H., Cerdan, O., Lefevre, I., Ayrault, S., 2014.
610 Renewed soil erosion and remobilisation of radioactive sediment in Fukushima coastal
611 rivers after the 2013 typhoons. Sci. Rep., 4.
612 Foster, I.D.L., Walling, D.E., 1994. Using reservoir deposits to reconstruct changing sediment
613 yields and sources in the catchment of the Old Mill Reservoir, South Devon, UK, Over
614 the past 50 years. . hydrological Sciences(39), 347 - 368.
615 Foster, I.D.L., Chapman, A.S., Hodgkinson, R.M., Jones, A.R., Lees, J.A., Turner, S.E., Scott,
616 M., 2003. Changing suspended sediment and particulate phosphorus loads and
617 pathways in underdrained lowland agricultural catchments; Herefordshire and
618 Worcestershire, U.K. Hydrobiologia, 494(1), 119-126.
619 Foucher, A., Salvador-Blanes, S., Desmet, M., Simonneau, A., Chapron, E., Evrard, O.,
620 Courp, T., Cerdan, O., Lefèvre, I., Adriaensen, H., Lecompte, F., 2015. Increased
621 erosion and sediment yield in a lowland catchment following the intensification of
622 agriculture (Louroux catchment, Loire Valley, France, 1950-2010). Anthropocene.
623 Froger, D., Moulin, J., Servant, J., 1994. Les terres de Gatines, Boischaud-Nord, Pays-Fort,
624 Touraine-Berry. Typologie des sols. Chambres d'agriculture du Cher, de l'Indre, de
625 l'Indre et Loire et du Loire et Cher.

626 Haddadchi, A., Ryder, D.S., Evrard, O., Olley, J., 2013. Sediment fingerprinting in fluvial
627 systems: review of tracers, sediment sources and mixing models. International Journal
628 of Sediment Research, 28(4), 560-578.
629 He, Q., Owens, P.N., 1995. Determination of suspended sediment provenance using caesium-
630 137, unsupported lead-210 and radium-226: a numerical mixing model approach.
631 Sediment and Water Quality in River Catchments, pp. 207–227.
632 He, Q., Walling, D.E., 1996. Interpreting particle size effects in the adsorption of 137Cs and
633 unsupported 210Pb by mineral soils and sediments. Journal of Environmental
634 Radioactivity, 30, pp. 117–137.
635 He, Q., Walling, D.E., 1997. The distribution of fallout 137Cs and 210Pb in undisturbed and
636 cultivated soils. Applied Radiation and Isotopes, 48(5), pp 677-690.
637 Horowitz, A.J., Elrick, K.A., 1987. The relation of stream sediment surface area, grain size
638 and composition to trace element chemistry. Applied Geochemistry, 2(4), pp. 437-451.
639 Horowitz, A.J., 2008. Determining annual suspended sediment and sediment-associated trace
640 element and nutrient fluxes. Science of The Total Environment, 400, 315.
641 Jagercikova, M., Evrard, O., Balesdent, J., Lefèvre, I., Cornu, S., 2014. Modeling the
642 migration of fallout radionuclides to quantify the contemporary transfer of fine
643 particles in Luvisol profiles under different land uses and farming practices. Soil and
644 Tillage Research, 140(0), pp. 82-97.
645 Jones, A., Panagos, P., Barcelo, S., Bouraoui, F., Bosco, C., Dewitte, O., Gardi, C., Erhard,
646 M., Hervás, J., Hiederer, R., Jeffery, S., Lükewille, A., Marmo, L., Montanarella, L.,
647 Olazábal, C., Petersen, J., Penizek, V., Strassburger, T., Tóth, G., Van Den Eeckhaut,
648 M., Van Liedekerke, M., Verheijen, F., Viestova, E., Yigini, Y., 2012. The state of soil
649 in Europe (SOER). JRC reference reports. Report 25186 EN.
650 http://ec.europa.eu/dgs/jrc/downloads/jrc_reference_report_2012_02_soil.pdf, 80 pp.
651 King, K.W., Fausey, N.R., Williams, M.R., 2014. Effect of subsurface drainage on
652 streamflow in an agricultural headwater watershed. Journal of Hydrology, 519, Part A,
653 pp 438-445.
654 Koiter, A.J., Owens, P.N., Petticrew, E.L., Lobb, D.A., 2013. The behavioural characteristics
655 of sediment properties and their implications for sediment fingerprinting as an
656 approach for identifying sediment sources in river basins. Earth-Science Reviews, 125,
657 24-42.
658 Kronvang, B., Laubel, A., Grant, R., 1997. Suspended sediment and particulate phosphorus
659 transport and delivery pathways in an arable catchment, Gelbaek stream, Denmark.
660 Hydrological Processes, 11(6), pp. 627-642.
661 Kronvang, B., Kronvang, B., Laubel, A., Larsen, S.E., Friberg, N., 2003. Pesticides and heavy
662 metals in Danish streambed sediment, The Interactions between Sediments and Water.
663 Developments in Hydrobiology. Springer Netherlands, pp. 93-101.
664 Laceby, J.P., Olley, J., 2015. An examination of geochemical modelling approaches to tracing
665 sediment sources incorporating distribution mixing and elemental correlations.
666 Hydrological Processes, n/a.
667 Laceby, J. P., Olley, J., Pietsch, T. J., Sheldon, F. and Bunn, S. E., 2015. Identifying subsoil
668 sediment sources with carbon and nitrogen stable isotope ratios. Hydrol.
669 Process., 29: 1956–1971
670 Macrae, M.L., English, M.C., Schiff, S.L., Stone, M., 2007. Intra-annual variability in the
671 contribution of tile drains to basin discharge and phosphorus export in a first-order
672 agricultural catchment. Agricultural Water Management, 92(3), pp 171-182.
673 Martinez-Carreras, N., Udelhoven, T., Krein, A., Gallart, F., Iffly, J.F., Ziebel, J., Hoffmann,
674 L., Pfister, L., Walling, D.E., 2010. The use of sediment colour measured by diffuse

675 reflectance spectrometry to determine sediment sources: Application to the Attert
676 River catchment (Luxembourg). Journal of Hydrology, 382, p 49-63.
677 Matisoff, G., Bonniwell, E.C., Whiting, P.J., 2002. Soil erosion and sediment sources in an
678 Ohio watershed using Beryllium-7, Cesium-137, and Lead-210. Journal of
679 Environmental Quality(31), 54-61.
680 Motha, J.A., Wallbrink, P.J., Hairsine, P.B., Grayson, R.B., 2002. Tracer properties of eroded
681 sediment and source material. Hydrological Processes, 16(10), pp 1983-2000.
682 Nakamura, F., Kameyama, S., Mizugaki, S., 2004. Rapid shrinkage of Kushiro Mire, the
683 largest mire in Japan, due to increased sedimentation associated with land-use
684 development in the catchment. CATENA, 55(2), 213.
685 Navratil, O., Evrard, O., Esteves, M., Legout, C., Ayrault, S., Némery, J., Mate-Marin, A.,
686 Ahmadi, M., Lefèvre, I., Poirel, A., Bonté, P., 2012. Temporal variability of
687 suspended sediment sources in an alpine catchment combining river/rainfall
688 monitoring and sediment fingerprinting. Earth Surface Processes and Landforms.
689 Olley, J., Caitcheon, G., 2000. Major element chemistry of sediments from the Darling-
690 Barwon river and its tributaries: implications for sediment and phosphorus sources.
691 Hydrological Processes, 14(7), 1159-1175.
692 Olley, J., Burton, J., Smolders, K., Pantus, F., Pietsch, T., 2013. The application of fallout
693 radionuclides to determine the dominant erosion process in water supply catchments
694 885-895.
695 Owens, P.N., Walling, D.E., 2002. The phosphorus content of fluvial sediment in rural and
696 industrialized river basins. Water Research, 36, pp. 685-701.
697 Owens, P.N., Batalla, R.J., Collins, A.J., Gomez, B., Hicks, D.M., Horowitz, A.J., Kondolf,
698 G.M., Marden, M., Page, M.J., Peacock, D.H., Petticrew, E.L., Salomons, W.,
699 Trustrum, N.A., 2005. Fine-grained sediment in river systems: environmental
700 significance and management issues. River Research and applications, 21(7), 693-717.
701 Oygarden, L., Kvaerner, J., Jenssen, P.D., 1997. Soil erosion via preferential flow to drainage
702 systems in clay soils. Geoderma, 76, pp 65-86.
703 Penven, M.-J., Muxart, T., 1995. Le drainage agricole : un rôle fondamental dans les
704 transferts d'eau et de matière. L'exemple du plateau briard. Annales de Géographie,
705 104(n° 581 - 582), 88 - 104 p.
706 Penven, M.-J., Muxart, T., Cosandey, C., Andreu, A., 2001. Contribution du drainage agricole
707 enterré à l'érosion des sols en région tempérée (BRIE). pp 128 - 144.
708 Pulley, S., Foster, I., Antunes, P., 2015. The uncertainties associated with sediment
709 fingerprinting suspended and recently deposited fluvial sediment in the Nene river
710 basin. Geomorphology, 228(0), pp. 303-319.
711 Rasplus, L., Macaire, J.J., Alcaydé, G., 1982. Carte géologique de Bléré au 1:5000, Editions
712 BRGM.
713 Russell, M.A., Walling, D.E., Hodgkinson, R.A., 2001. Suspended sediment sources in two
714 small lowland agricultural catchments in the UK. Journal of Hydrology, 252, p 1-24.
715 Sakaguchi, A., Yamamoto, M., Sasaki, K., Kashiwaya, K., 2006. Uranium and Thorium
716 Isotope Distribution in an Offshore Bottom Sediment Core of the Selenga Delta, Lake
717 Baikal, Siberia. Journal of Paleolimnology, 35(4), 807-818.
718 Sharma, A., Tiwari, K., Bhadoria, P.B.S., 2011. Effect of land use land cover change on soil
719 erosion potential in an agricultural watershed. Environmental Monitoring and
720 Assessment, 173(1-4), 789-801.
721 Smith, H.G., Blake, W.H., 2014. Sediment fingerprinting in agricultural catchments: A
722 critical re-examination of source discrimination and data corrections. Geomorphology,
723 204(0), 177.

724 Sogon, S., 1999. Erosion des sols cultivés et transport des matières en suspension dans un
725 bassin versant de Brie. Application des traceurs radioactifs naturels et magnétiques.
726 Université Paris1 - Panthéon-Sorbonne. Thèse, 305 p.
727 Sogon, S., Penven, M.J., Bonte, P., Muxart, T., 1999. Estimation of sediment yield and soil
728 loss using suspended sediment load and 137Cs measurements on agricultural land,
729 Brie Plateau, France. Hydrobiologia, 410(0), 251-261.
730 Wallbrink, P.J., Murray, A.S., 1996. Distribution and Variability of 7Be in Soils Under
731 Different Surface Cover Conditions and its Potential for Describing Soil
732 Redistribution Processes. Water Resources Research, 32(2), pp 467-476.
733 Wallbrink, P.J., Olley, J.M., Murray, A.S., Olive, L.J., 1996. The contribution of subsoil to
734 sediment yield in the Murrumbidgee River basin, New South Wales, Australia.
735 Erosion and sediment yield: global and regional perspectives. (Proceedings Exeter
736 symposium, 1996). IAHS Publication, 236, pp. 347–355.
737 Wallbrink, P.J., 2004. Quantifying the erosion processes and land-uses which dominate fine
738 sediment supply to Moreton Bay, Southeast Queensland, Australia. Journal of
739 Environmental Radioactivity, 76.
740 Walling, D.E., Woodward, J.C., Nicholas, A.P., 1993. A multi-parameter approach to
741 fingerprinting suspended-sediment sources, IAHS publication.
742 Walling, D.E., Russell, M.A., Hodgkinson, R.A., Zhang, Y., 2002. Establishing sediment
743 budgets for two small lowland agricultural catchments in the UK. CATENA, 47(4),
744 323-353.
745 Walling, D.E., Owens, P.N., Foster, I.D.L., Lees, J.A., 2003. Changes in the fine sediment
746 dynamics of the Ouse and Tweed basins in the UK over the last 100–150 years.
747 Hydrological Processes, 17(16), 3245.
748 Walling, D.E., 2005. Tracing suspended sediment sources in catchments and river systems.
749 Science of The Total Environment, 344, pp 159-184.
750 Walling, D.E., Collins, A.L., 2005. Sediment Budgets, IAHS Press, Wallingford 123–133.
751 Wood, P.J., Armitage, P.D., 1997. Biological Effects of Fine Sediment in the Lotic
752 Environment. Environmental Management, 21(2), 203-217.
753
754
755
756
757 Figure captions:
758
759
760 Fig. 1. Catchment and sampling location map with, A) the location of the study site in the Loire River
761 basin, and B) the Louroux pond catchment with source sample locations and river monitoring sites
762 (S1: Beaulieu River, S2: Grand Bray River, S3: Masnier River, S4: Picarderie River, S5: Conteraye
763 River and D1–3: drain stations, H: Hillslope sediment samples collected during runoff events).
764
765 Fig. 2. ^{137}Cs activities in multiple particle size fractions, (bulk soil and fractions ranging 63–50, 50–20,
766 or <20 µm) and suspended sediment (*SS*).
767
768 Fig. 3. Relationship between $^{210}Pb_{ex}$ and ^{137}Cs for surface and subsurface sources along with in-stream
769 sediments.
770

Fig. 4. Relationship between measured and corrected ^{137}Cs activities for the surface and subsurface samples using the *SSA* (A) and *Th* (B) correcting factors. Error bars represent analytical uncertainties on radionuclide activities (1 sigma).

Fig. 5. Relationship between $^{210}Pb_{ex}$ and ^{137}Cs for surface and subsurface sources along with in-stream sediments after the *SSA* (A) and *Th* (B) particle size corrections.

Fig. 6. Probability plots characterizing surface and subsurface sample distributions with the *SSA* (A) and *Th* (B) particle size corrections. The probabilities were generated for each source with 2500 Latin hypercube samples from each source distribution.

Fig. 7. Probability plots for ^{137}Cs activity concentrations including sediment samples (black squares) collected from the monitoring sites. In each case, probabilities were generated with 2500 Latin hypercube samples from the source and sediment distributions as well as the mixture distribution. Error bars represent analytical uncertainties of sediment samples equivalent to one standard error of the mean. The solid line is the subsurface source distribution, the dashed line is the surface source distribution and the dotted line is the distribution of sediment from each monitoring station.

Fig. 8. Probability plots for ^{137}Cs activity concentrations including sediment samples (black circles) collected during the six sampling survey (SSE1: 09 Sept 2013; SSE2: 30 Dec 2013; SSE3: 29 Jan 2014; SSE4: 13 Feb 2014; SSE5: 4 Apr 2014; SSE6: 30 Apr 2014). In each case, probabilities were generated with 2500 Latin hypercube samples from the source and sediment distributions as well as the mixture distribution. Error bars represent analytical uncertainties of sediment samples equivalent to one standard error of the mean. The solid line is the subsurface source distribution, the dashed line is the surface source distribution and the dotted line is the distribution of sediment from each event sampled.

Fig. 9. Probability plots for ^{137}Cs activity concentrations including the core and tile drainage network samples (black circles). In each case, probabilities were generated with 2500 Latin hypercube samples from the source and sediment distributions as well as the mixture distribution. Error bars represent analytical uncertainties of sediment samples equivalent to one standard error of the mean. The solid line is the subsurface source distribution, the dashed line is the surface source distribution and the dotted line is the distribution of sediment from core and tile drainage network.

Table captions:

807 Table 1. Summary of ^{137}Cs activities (Bq kg^{-1}) of the potential sources with the different correction
808 techniques (w/o corr: without correction, *SSA*: surface specific correction, *Th*: Thorium correction).
809
810 Table 2. Summary of mean ^{137}Cs activities and the standard deviation (σ) (Bq kg^{-1}) for the in-stream
811 and drain samples at each monitoring station during flood events.
812
813 Table 3. Details of modeling results for surface and subsurface contributions.
814
815

Table 1

Statistic	Subsoil			Surface		
	w/o corr.	*SSA*	*Th*	*w/o corr.*	*SSA*	*Th*
Mean	1.3	1.7	1.8	3.2	10.0	11.2
Standard deviation	1.0	1.9	2.2	1.4	4.2	8.3
Mediane	1.0	1.3	0.9	2.9	9.3	9.3
Minimum	0.0	-0.7	0.0	1.0	3.7	0.8
Maximum	3.1	5.1	6.5	7.9	23.8	35.5

Table 2

	Date	^{137}Cs	σ
Station 1	09/09/2013	8.6	0.7
	30/12/2013	21.3	4.2
	29/01/2014	20.3	1.6
	13/02/2014	16.9	0.8
	04/04/2014	10.3	3.2
Station 2	09/09/2013	6.0	0.6
	30/12/2013	24.6	4.4
	29/01/2014	18.3	2.1
	13/02/2014	17.8	1.0
Station 3	30/12/2013	6.3	2.4
	29/01/2014	25.1	3.1
	13/02/2014	14.3	0.9
	04/04/2014	30.2	13.2
	30/04/2014	0.0	17.3
Station 4	09/09/2013	7.1	1.1
	30/12/2013	11.5	5.1
	29/01/2014	23.1	2.4
	13/02/2014	15.4	0.8
	30/04/2014	31.3	8.6
Station 5	09/09/2013	6.1	1.0
	30/12/2013	25.5	5.3
	29/01/2014	36.7	4.7
	13/02/2014	21.3	1.8
	04/04/2014	18.8	5.4
	30/04/2014	24.4	7.7
D1	30/12/2013	13.4	2.3
	29/01/2014	23.5	4.1
D2	16/01/2013	8.6	0.3
D3	30/12/2013	30.6	7.5
	29/01/2014	26.1	2.3

Table 3

Type	Surface contribution (%) and standard error (%)			
	SSA		*Th*	
Average sample	99	± 2	94	± 1.5
Sediment Core	99	± 1.5	97	± 6.7
Drain sediment	99	± 2	99	± 2.5
Station 1	99	± 1	96	± 2
Station 2	98	± 1.6	95	± 1.5
Station 3	99	± 1	99	± 1
Station 4	99	± 1.2	99	± 1
Station 5	99	± 1.1	99	± 1.2
SSE1- 09 sep 13	49	± 3.5	40	± 2
SSE2- 30 dec 13	98	± 1	99	± 1.4
SSE3- 29 jan 14	99	± 1	99	± 1
SSE4- 13 feb 14	99	± 2	98	± 1.5
SSE5- 04 apr 14	99	± 1	99	± 2
SSE6- 30 apr 14	98	± 1.5	99	± 3

Figure (Color)

Fig. 1

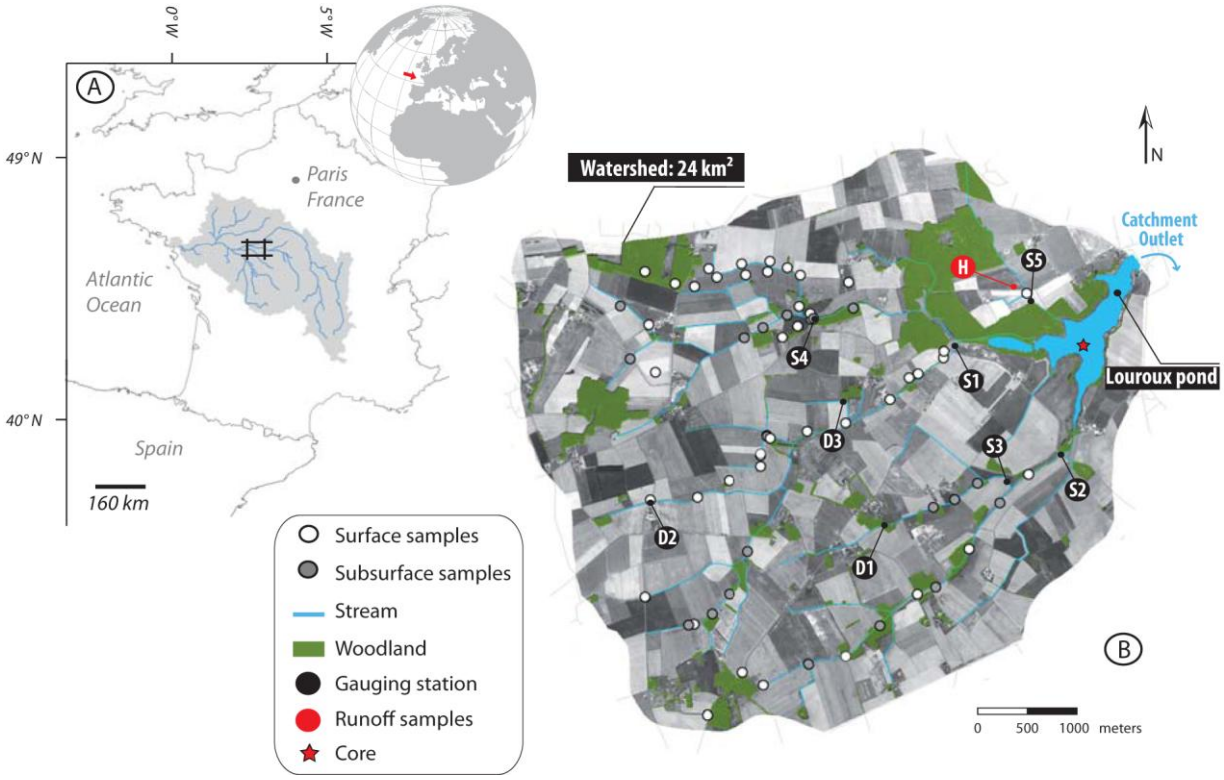

Fig. 2

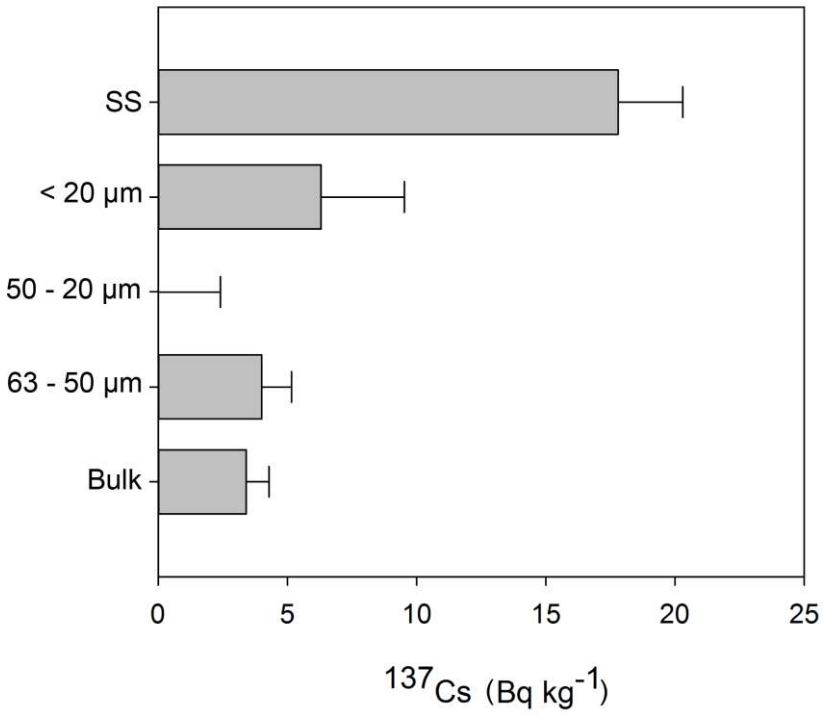

Fig. 3

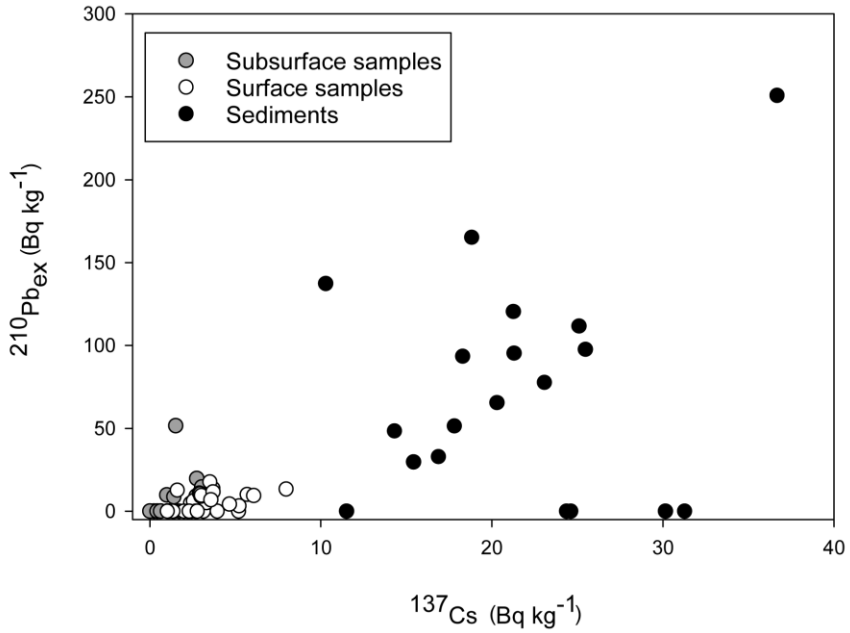
Subsurface samples
Surface samples
Sediments
$^{210}Pb_{ex}$ (Bq kg^{-1})
^{137}Cs (Bq kg^{-1})
0
50
100
150
200
250
300
0
10
20
30
40

Fig. 4

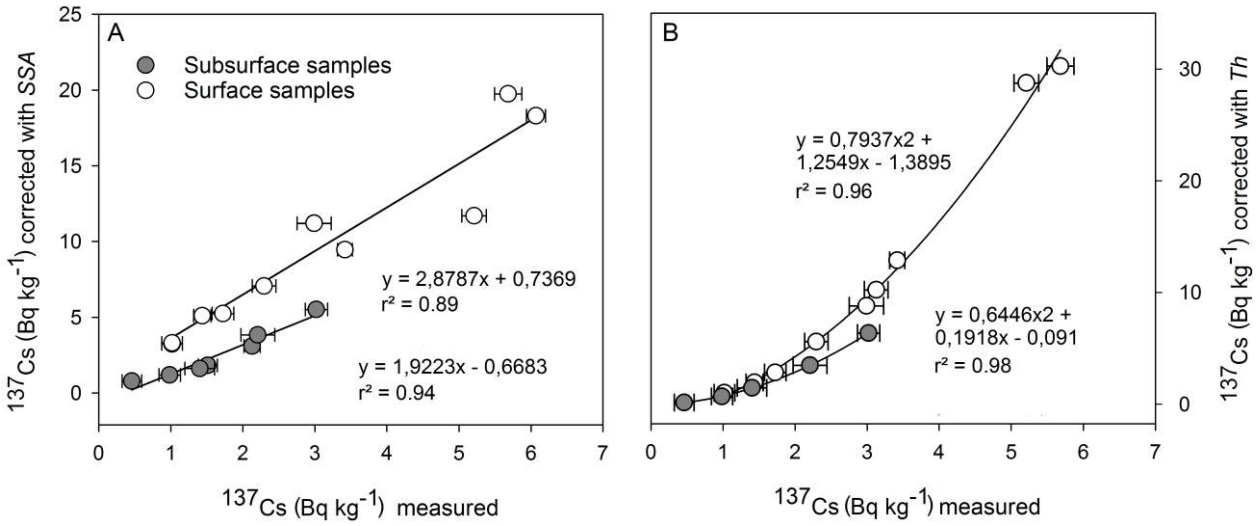
A
Subsurface samples
Surface samples
y = 2,8787x + 0,7369
r² = 0.89
y = 1,9223x - 0,6683
r² = 0.94
137Cs (Bq kg-1) corrected with SSA
137Cs (Bq kg-1) measured
B
y = 0,7937x2 +
1,2549x - 1,3895
r² = 0.96
y = 0,6446x2 +
0,1918x - 0,091
r² = 0.98
137Cs (Bq kg-1) corrected with Th
137Cs (Bq kg-1) measured

Fig. 5

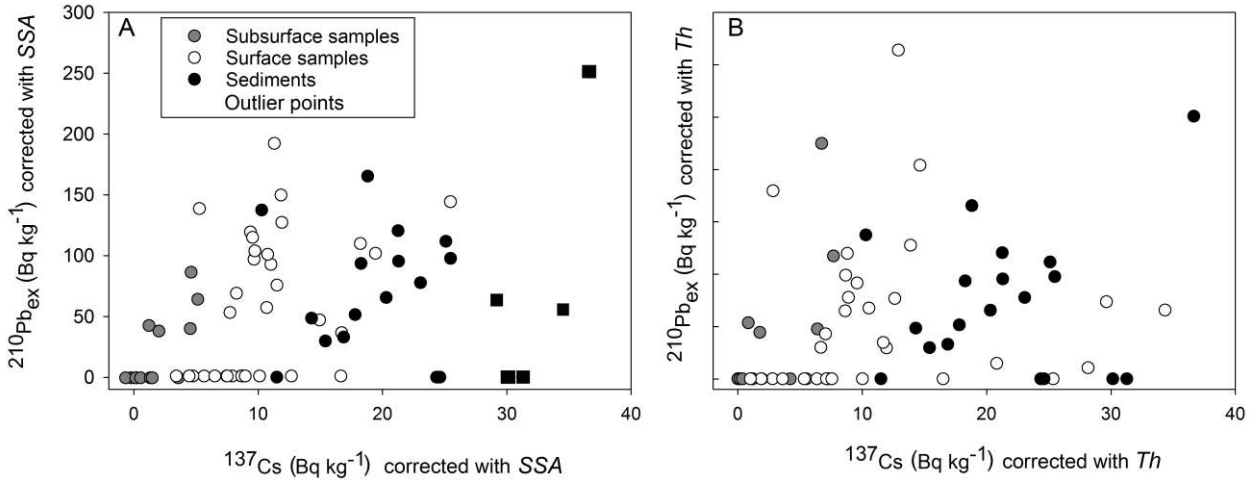
A
Subsurface samples
Surface samples
Sediments
Outlier points
$^{210}Pb_{ex}$ (Bq kg^{-1}) corrected with *SSA*
^{137}Cs (Bq kg^{-1}) corrected with *SSA*
B
$^{210}Pb_{ex}$ (Bq kg^{-1}) corrected with *Th*
^{137}Cs (Bq kg^{-1}) corrected with *Th*

Fig. 6

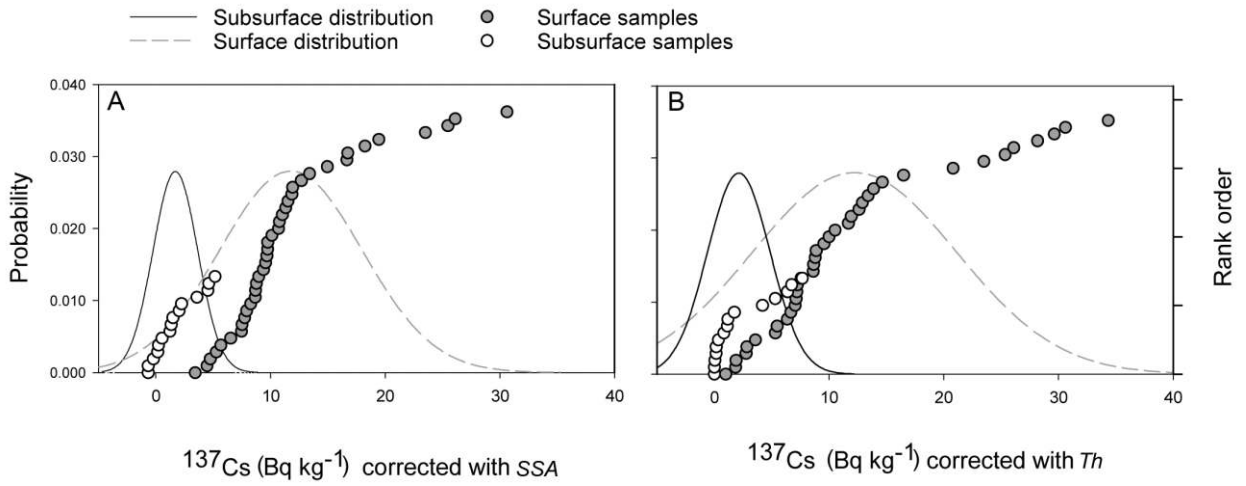
Subsurface distribution
Surface distribution
Surface samples
Subsurface samples
A
B
Probability
Rank order
0.040
0.030
0.020
0.010
0.000
0
10
20
30
40
137Cs (Bq kg-1) corrected with SSA
137Cs (Bq kg-1) corrected with Th

Fig. 7

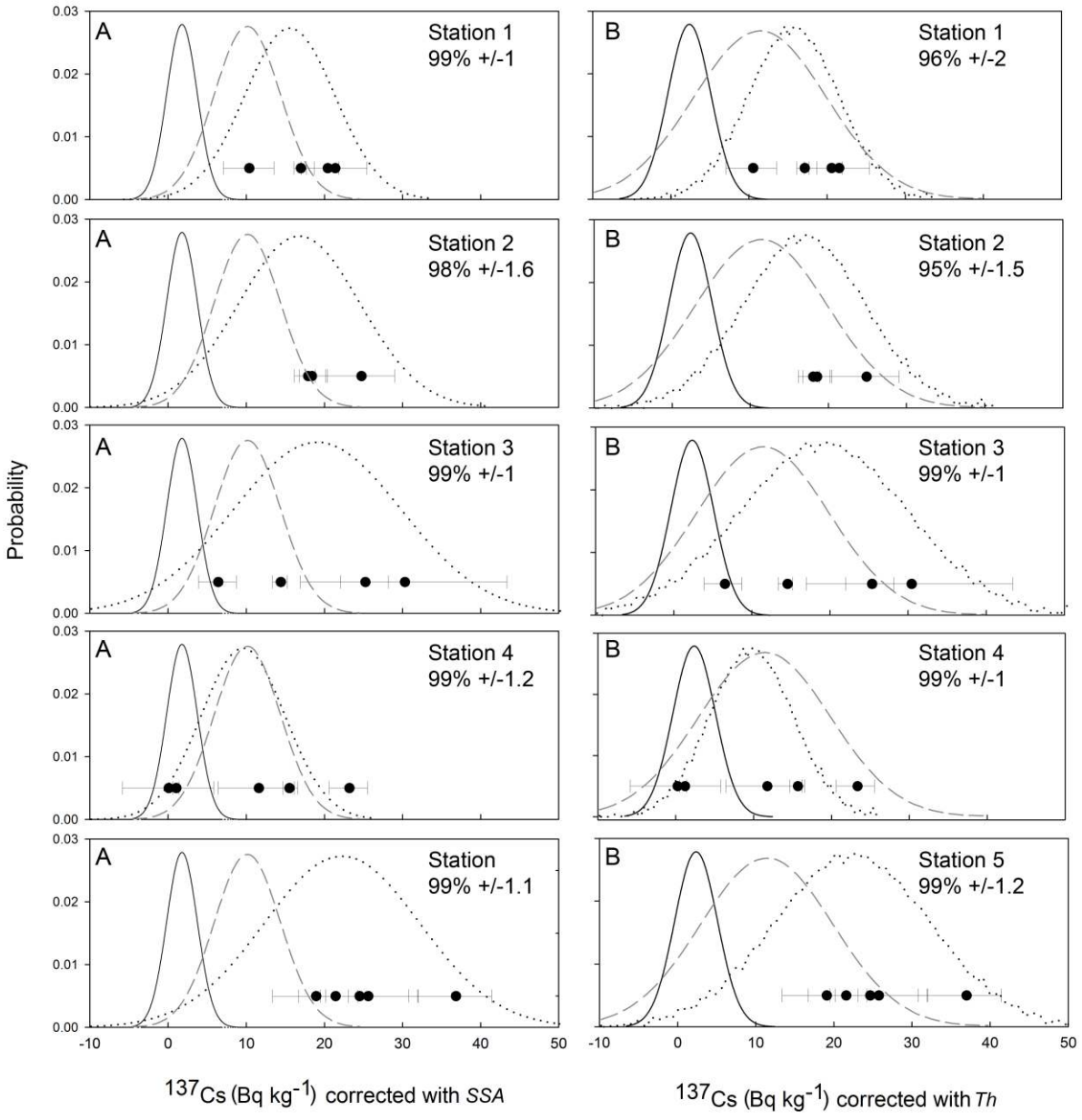
A
Station 1
99% +/-1
B
Station 1
96% +/-2
A
Station 2
98% +/-1.6
B
Station 2
95% +/-1.5
A
Station 3
99% +/-1
B
Station 3
99% +/-1
A
Station 4
99% +/-1.2
B
Station 4
99% +/-1
A
Station
99% +/-1.1
B
Station 5
99% +/-1.2
Probability
0.03
0.02
0.01
0.00
-10
0
10
20
30
40
50
137Cs (Bq kg-1) corrected with SSA
137Cs (Bq kg-1) corrected with Th

Fig. 8

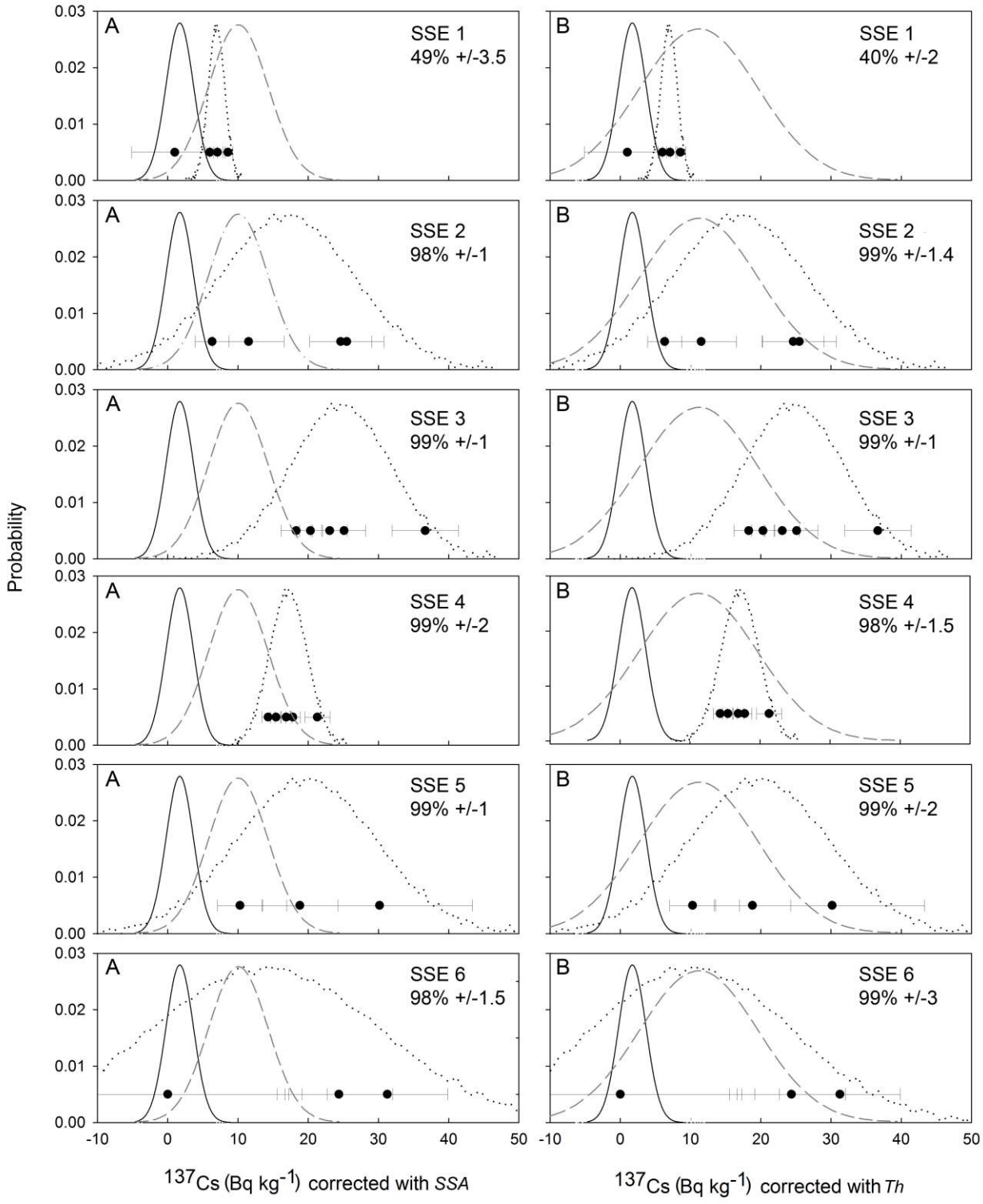
A
SSE 1
49% +/-3.5
B
SSE 1
40% +/-2
A
SSE 2
98% +/-1
B
SSE 2
99% +/-1.4
A
SSE 3
99% +/-1
B
SSE 3
99% +/-1
A
SSE 4
99% +/-2
B
SSE 4
98% +/-1.5
A
SSE 5
99% +/-1
B
SSE 5
99% +/-2
A
SSE 6
98% +/-1.5
B
SSE 6
99% +/-3
Probability
0.03
0.02
0.01
0.00
-10
0
10
20
30
40
50
137Cs (Bq kg-1) corrected with SSA
137Cs (Bq kg-1) corrected with Th

Fig. 9

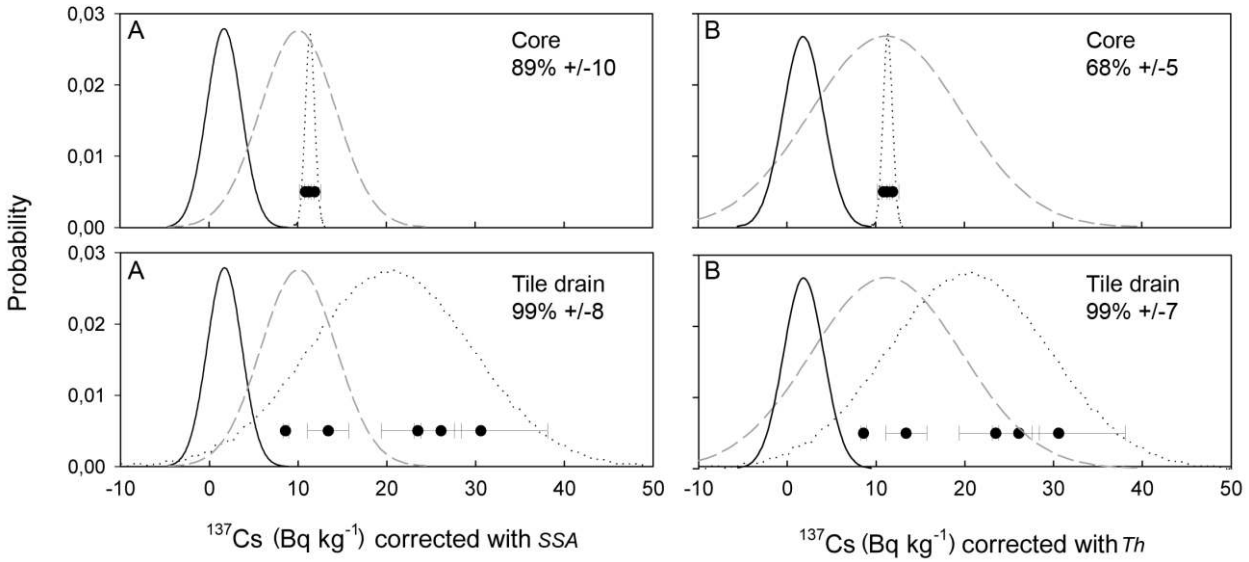
A
Core
89% +/-10
B
Core
68% +/-5
A
Tile drain
99% +/-8
B
Tile drain
99% +/-7
Probability
0,03
0,02
0,01
0,00
-10
0
10
20
30
40
50
137Cs (Bq kg-1) corrected with SSA
137Cs (Bq kg-1) corrected with Th

Figure (Greyscale)

Fig. 1

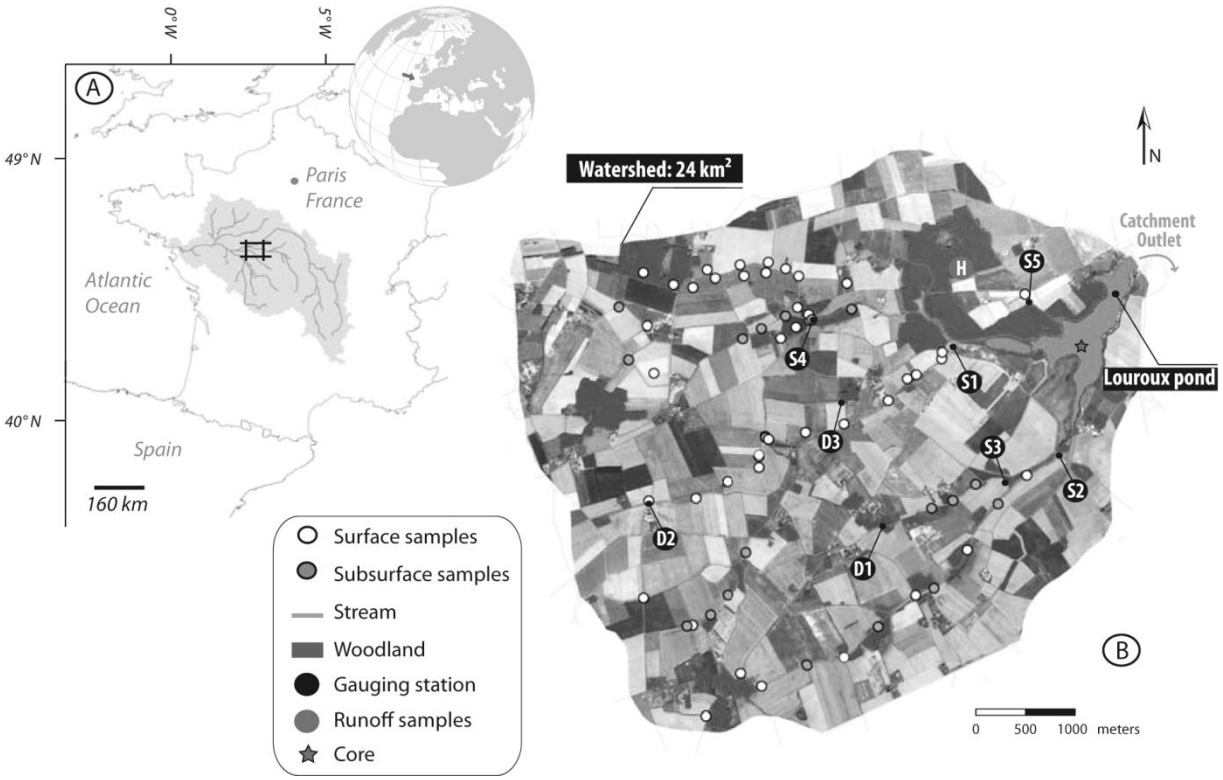

Fig. 2

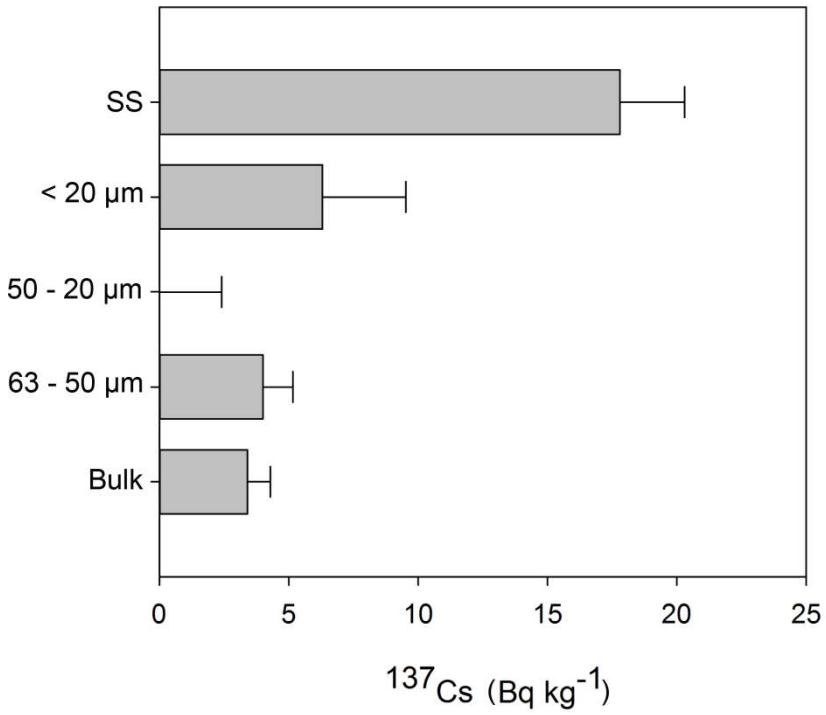

Fig. 3

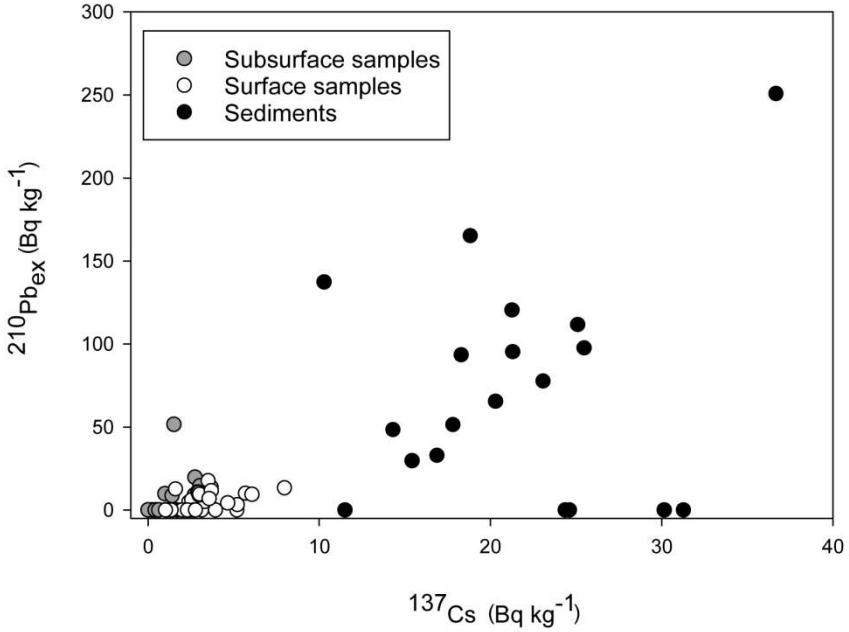
Subsurface samples
Surface samples
Sediments
300
250
200
150
100
50
0
0
10
20
30
40
$^{210}Pb_{ex}$ (Bq kg^{-1})
^{137}Cs (Bq kg^{-1})

Fig. 4

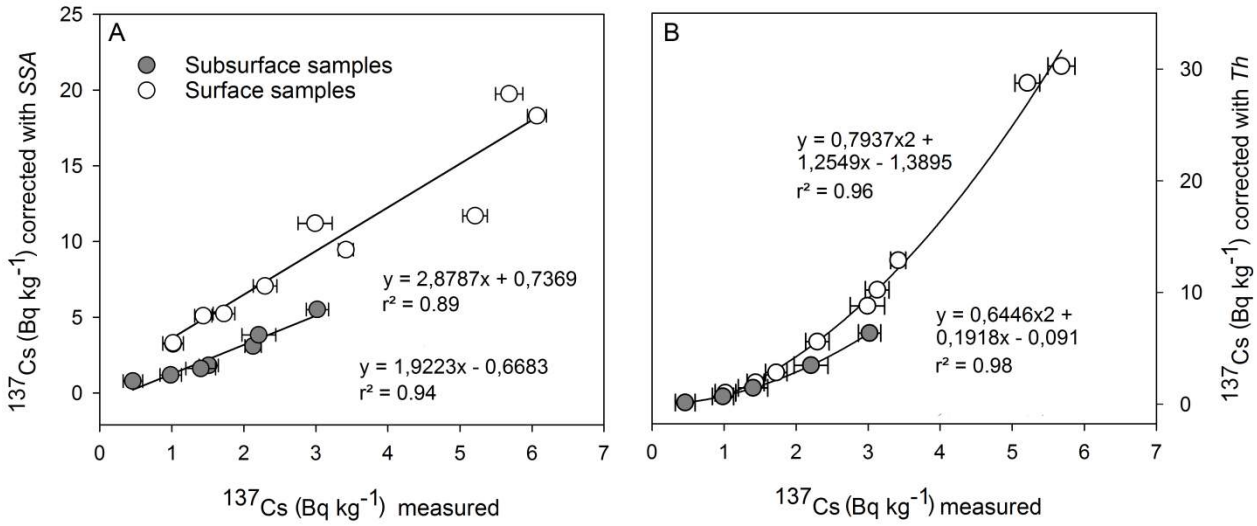
A
Subsurface samples
Surface samples
y = 2,8787x + 0,7369
r² = 0.89
y = 1,9223x - 0,6683
r² = 0.94
137Cs (Bq kg-1) corrected with SSA
137Cs (Bq kg-1) measured
B
y = 0,7937x2 +
1,2549x - 1,3895
r² = 0.96
y = 0,6446x2 +
0,1918x - 0,091
r² = 0.98
137Cs (Bq kg-1) corrected with Th
137Cs (Bq kg-1) measured

Fig. 5

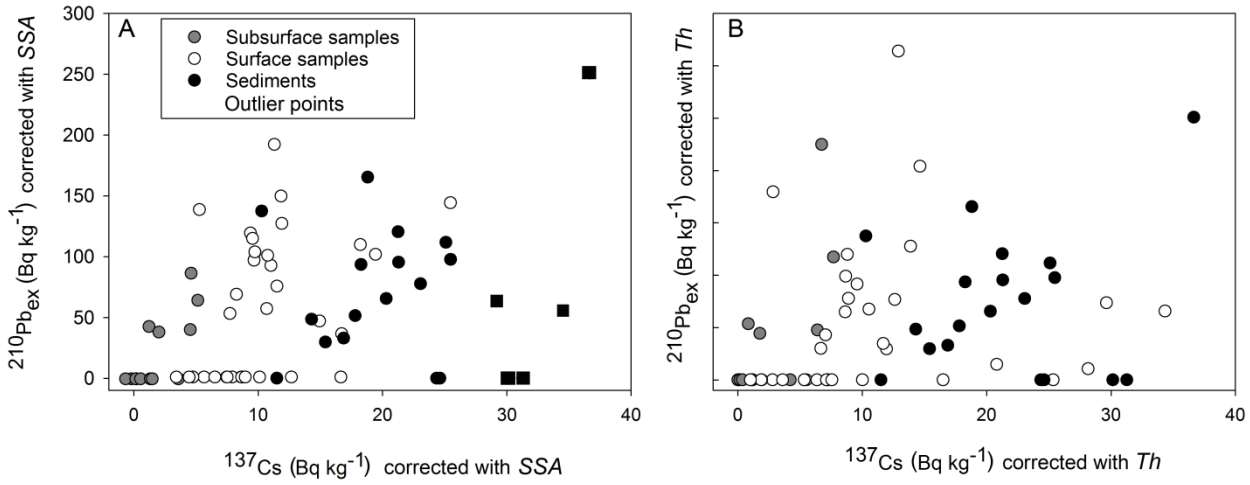
A
Subsurface samples
Surface samples
Sediments
Outlier points
$^{210}Pb_{ex}$ (Bq kg^{-1}) corrected with *SSA*
^{137}Cs (Bq kg^{-1}) corrected with *SSA*
B
$^{210}Pb_{ex}$ (Bq kg^{-1}) corrected with *Th*
^{137}Cs (Bq kg^{-1}) corrected with *Th*

Fig. 6

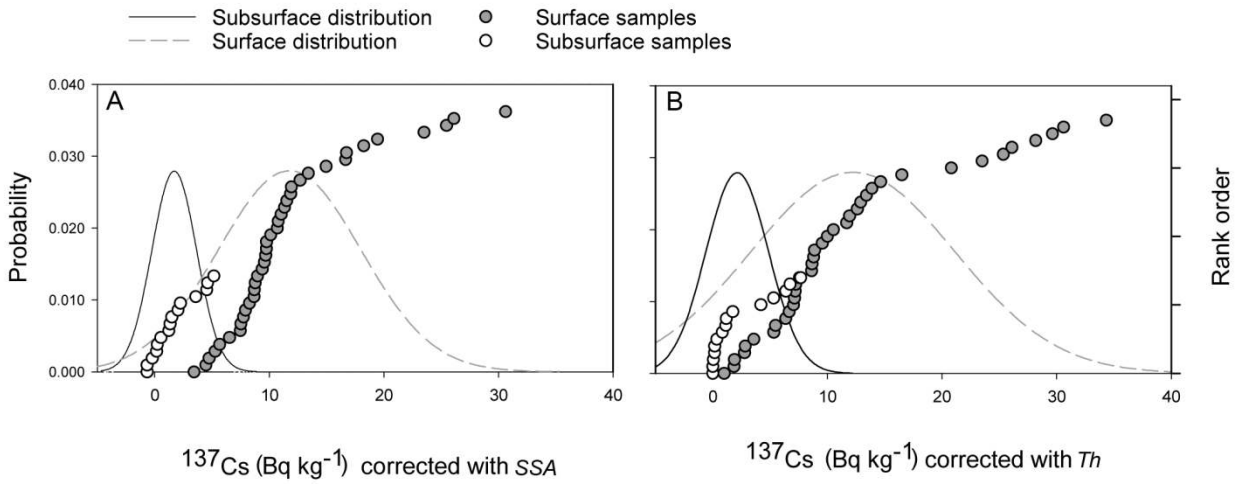
Subsurface distribution
Surface distribution
Surface samples
Subsurface samples
A
B
Probability
Rank order
0.040
0.030
0.020
0.010
0.000
0
10
20
30
40
137Cs (Bq kg-1) corrected with SSA
137Cs (Bq kg-1) corrected with Th

Fig. 7

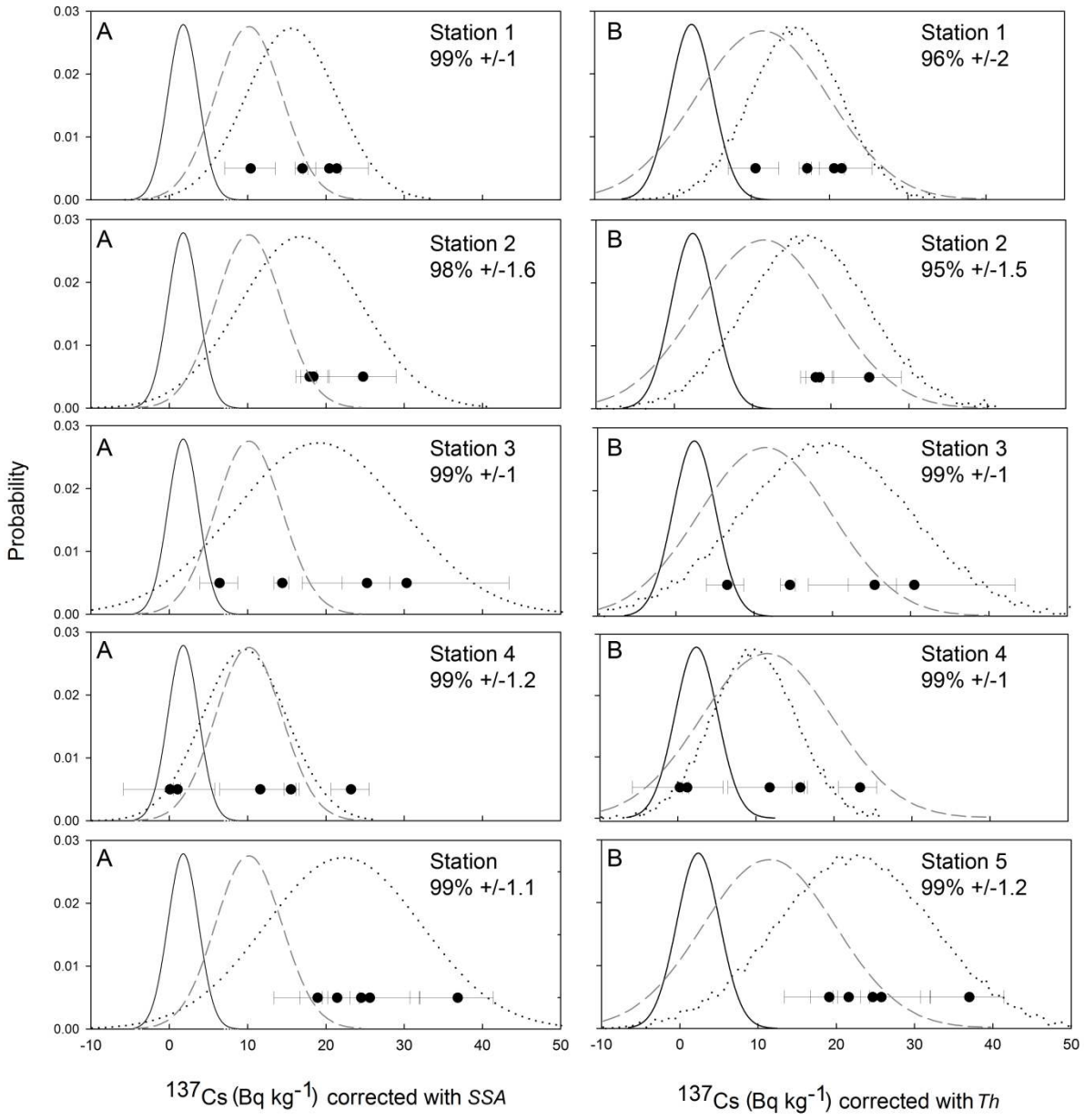
A
Station 1
99% +/-1
B
Station 1
96% +/-2
A
Station 2
98% +/-1.6
B
Station 2
95% +/-1.5
A
Station 3
99% +/-1
B
Station 3
99% +/-1
A
Station 4
99% +/-1.2
B
Station 4
99% +/-1
A
Station
99% +/-1.1
B
Station 5
99% +/-1.2
Probability
0.03
0.02
0.01
0.00
-10
0
10
20
30
40
50
137Cs (Bq kg-1) corrected with SSA
137Cs (Bq kg-1) corrected with Th

Fig. 8

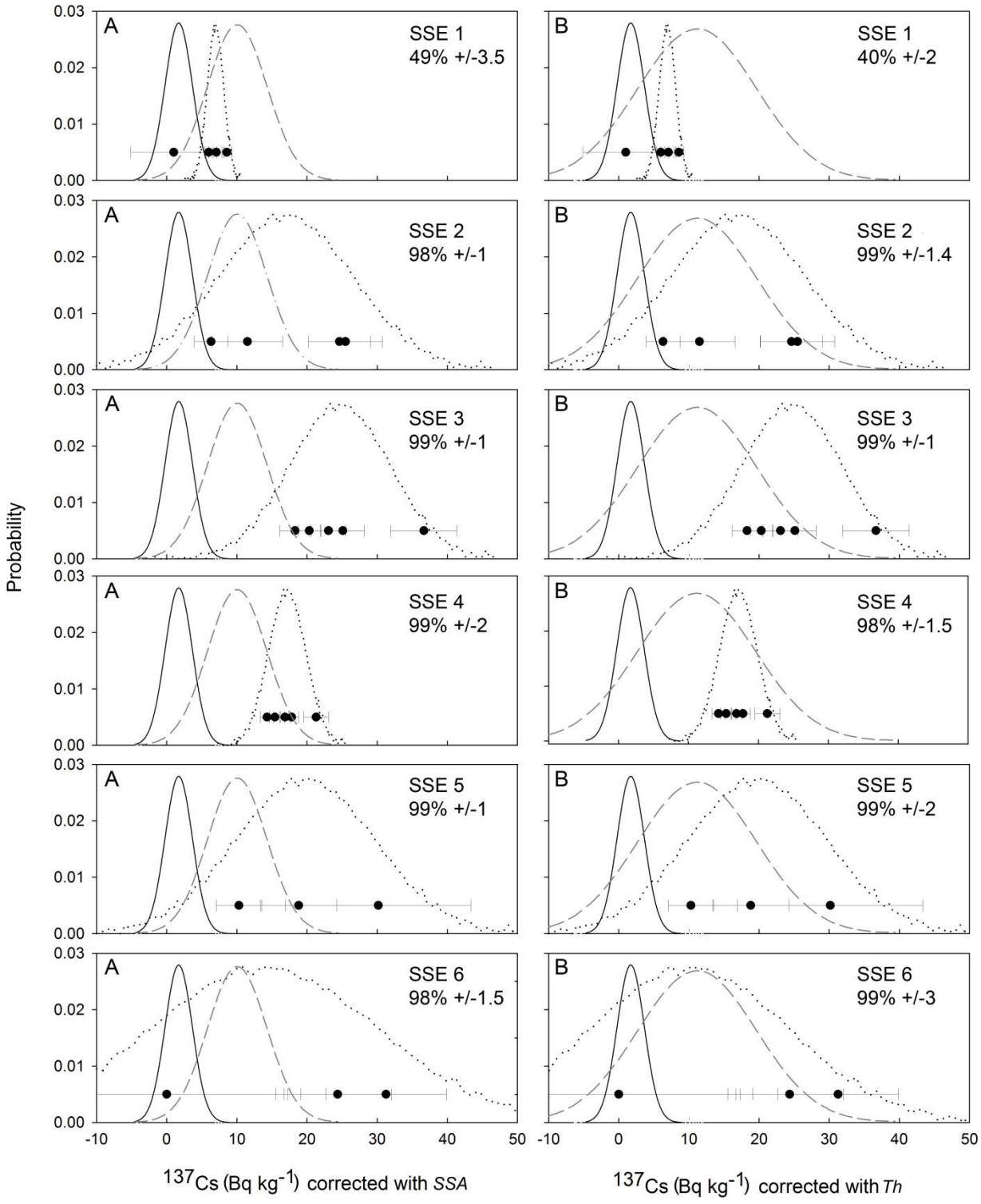
A
SSE 1
49% +/-3.5
B
SSE 1
40% +/-2
A
SSE 2
98% +/-1
B
SSE 2
99% +/-1.4
A
SSE 3
99% +/-1
B
SSE 3
99% +/-1
A
SSE 4
99% +/-2
B
SSE 4
98% +/-1.5
A
SSE 5
99% +/-1
B
SSE 5
99% +/-2
A
SSE 6
98% +/-1.5
B
SSE 6
99% +/-3
Probability
0.03
0.02
0.01
0.00
-10
0
10
20
30
40
50
137Cs (Bq kg-1) corrected with SSA
137Cs (Bq kg-1) corrected with Th

Fig. 9

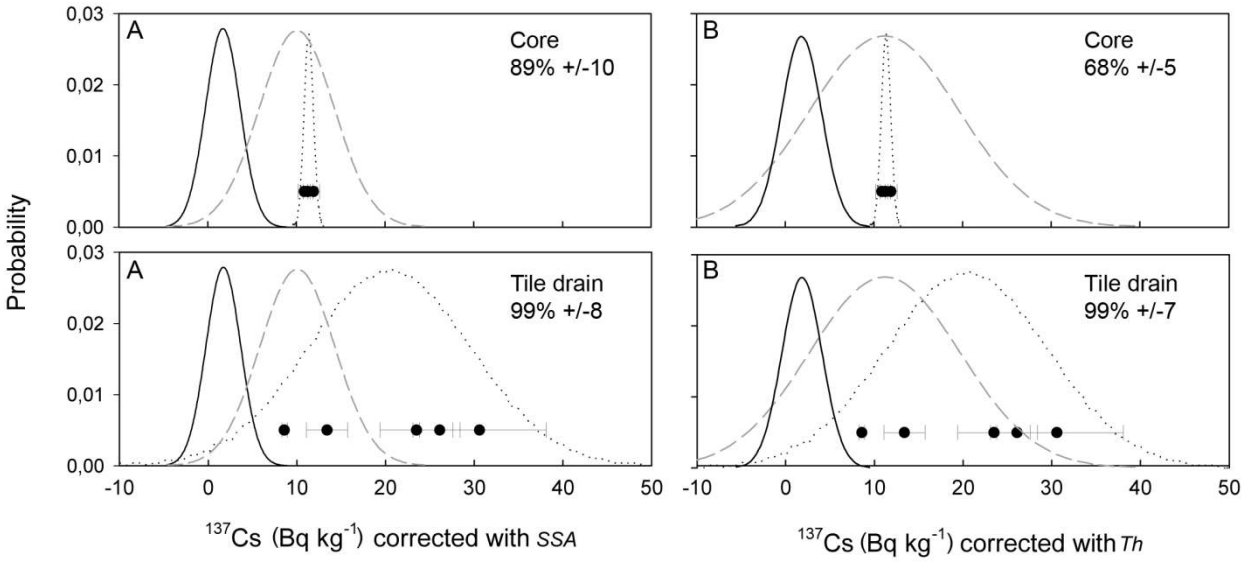
A
Core
89% +/-10
B
Core
68% +/-5
A
Tile drain
99% +/-8
B
Tile drain
99% +/-7
Probability
0,03
0,02
0,01
0,00
-10
0
10
20
30
40
50
137Cs (Bq kg-1) corrected with SSA
137Cs (Bq kg-1) corrected with Th